CHARLES UNIVERSITY IN PRAGUE
Faculty of Science

Department of physical and macromolecular chemistry

Vladimír Ďorďovič

ASOCIAČNÍ CHOVÁNÍ KARBORANŮ A JEJICH INTERAKCE S POLYMERY V ROZTOCÍCH

ASSOCIATION BEHAVIOUR OF CARBORANES AND THEIR INTERACTIONS WITH POLYMERS IN SOLUTIONS

Diploma Thesis

Supervisor: RNDr. Pavel Matějíček, Ph.D.

Prague 2013

ABSTRAKT

Tato diplomová práce se zabývá chováním kobalt bis(dikarbollid)u a jeho derivátů obsahujících polyethylenoxidový linker ve vodném roztoku a roztoku soli a jejich interakcí s některými biokompatibilními polymery. V této práci byl použit diblokový kopolymer poly(ethylenoxid)-*block*-poly(2-ethyl oxazolin), PEO-PEOX, triblokový kopolymer poly(2-ethyl oxazolin)-*block*-poly(ethylenoxid)-*block*-poly(2-ethyl oxazolin), PEOX-PEO-PEOX a hvězdicový kopolymer 4-ramenný poly(ethylenoxid)-*block*-poly(2-methyl oxazolin), 4-ramenný PEO-PMOX. Rozpustnost a změna hydrodynamického poloměru metallakarboranových částic byla studována v závislosti na kationtu příslušné soli. Rozpustnost i velikost částic se mění v závislosti na protiontu metallakarboranu a taky na délce a typu PEG linkeru sloučeniny karboranu. Kobalt bis(dikarbollid) i jeho deriváty tvoří v roztoku s polymery částice tvořené komplexem polymer/caborane. Přídavek polymeru zvyšuje rozpustnost karboranů a ve většině případu snižuje velikost částic v roztoku. Tyto systémy byli studovány pomocí rozptylových technik, UV-VIS spektroskopie, ITC, NMR a SAXS.

ABSTRACT

This diploma thesis deals with the behavior of cobalt bis(dicarbollide) and its derivatives containing polyethylene oxide linkers in aqueous and salted solution and their interactions with some biocompatible block copolymers. In this study we chose diblock copolymer poly(ethylene oxide)-*block*-poly(2-ethyl oxazoline), PEO-PEOX, triblock copolymer poly(2-ethyl oxazoline)-*block*-poly(ethylene oxide)-*block*-poly(2-ethyl oxazoline), PEOX-PEO-PEOX and starlike polymer 4-arm poly(ethylene oxide)-*block*-poly(2-methyl oxazoline), 4-arm PEO-PMOX. Solubility and change of hydrodynamic radius of metallacarborane particles depending on the cation of corresponding salt solution was studied. Solubility and size of particles changes depending on counterion of metallacarborane and also on the length and type of PEG linker of carborane compound. In solutions with polymer cobalt bis(dicarbollide) and his conjugates form particles composed of complex polymer/caborane. Adding polymer increase solubility of carborane and in most cases it decreases the size of particles in solution. These systems were studied by means of light scattering, UV-VIS spectroscopy, ITC, NMR and SAXS.

I declare that I have elaborated the thesis on my own. If already published results are used, they are included in the list of references. I agree with lending the thesis to anyone who may be interested. It is not substantially the same as any work that has been or is being submitted to any other University for any degree, diploma or any other qualification.

Prague, 13.4.2013

.....

Signature

I would like to thank to my supervisor RNDr. Pavel Matějíček, Ph.D. for his personal guidance, constant assistance, inspiring discussions, valuable comments and suggestions and his patience with my many mistakes. I would also like to thank to Ing. Mariusz Uchman, Ph.D. for ITC measurements and Alexander Zhigunov, Ph.D. for SAXS measurements.

Obsah

ABBREVIATIONS

AFM atomic force microscopy

ATP adenosine-5'-triphosphate

BNCS boron neutron capture synovectomy

BNCT boron neutron capture therapy

CryoTEM cryogenic transmission electron microscopy

DLS dynamic light scattering

DHBC double hydrophilic block copolymer

HIV human immunodeficiency virus

ITC isothermal titration calorimetry

MRI magnetic resonance imaging

NMR nuclear magnetic resonance

PEG poly(ethylene glycol)

PEO poly(ethylene oxide)

PEOX poly(2-ethyl oxazoline)

PFG-NMR pulsed-field gradient nuclear magnetic resonance

PMA poly(methyl acrylate)

PMOX poly(2-methyl oxazoline)

PNIPAM poly(N-isopropylacrylamide)

R_H hydrodynamic radius

SLS static light scattering

SAXS small angle X-ray scattering

TEM transmission electron microscopy

UV-Vis ultraviolet–visible

1 MOTIVATION OF THE STUDY AND AIM OF THE THESIS

Carboranes and metallacarboranes have been a subject of intense research for over 50 years and are interesting compounds from both the fundamental and applied research. They have been attracting interest of a number of research teams for quite a long time but only recently an exceptionally efficient inhibition of HIV activity by cobalt bis(dicarbollide) derivatives was discovered. This medical application led to the extensive study of metallacarborane compounds. The aggregation of metallacarboranes in aqueous solutions contributes to the inhibition efficiency and this was the first stimulus for general research of metallacarborane solutions relating to this work. From the point of view of medical applications, the biggest challenge is the preparation of a thermodynamically stable dispersion of sparingly soluble boron-containing compounds in water, which would retain the biochemical activity. Further research revealed that the solubility in water can be increased by adding of suitable excipient, such as block copolymers, which has found a number of advanced applications in drug carrier vessels in targeted delivery systems and controlled drug release.

This study is focused on characterization of the aqueous solution of cobalt bis(dicarbollide) anion, **1**, and its various conjugates. One of the aims was to prepare stable nanoparticles with high loading capacity of cobaltacarboranes suitable for drug delivery. For this purpose biocompatible diblock hydrophilic copolymers containing poly(ethylene oxide) and poly(alkyl oxazoline) were used. The study is also aimed to characterize solutions by comparing solubility and behavior of aggregation. The study of solutions of **1** with PEO-PEOX was deeper as the results of previous research. Another goal was the study of influence of counterions of metallacarboranes and cations of salt on behavior in salt solution with and without polymers as well. These systems were studied by scattering techniques, spectroscopy and calorimetry.

2 INTRODUCTION

2.1 BORON CHEMISTRY

All life is derived ultimately from the element carbon, which lies next to boron in the periodic table of elements. Boron compounds not only share some similarities with carbon but also have important differences. It is the combination of these similarities and differences that give boron its unique potential in medicine. The important similarity is that boron, like carbon, combines with hydrogen to form stable compounds that can participate in biochemical reactions and interactions. The key difference is that these compounds have distinctive geometrical shapes and electronic charge distributions with greater 3D complexity than their carbon-based equivalents. While organic carbon molecules tend to comprise rings and chains, boron hydrides are made up of clusters and cages. This 3D structure makes it possible to design molecules with specific charge distributions by varying their internal structure, and this in turn brings the potential to tune how each part of the structure relates to water molecules which corresponds with their hydrophobic or hydrophilic character. In living organisms, at intracellular pH, nearly all natural boron exists as boric acid, which behaves as a Lewis acid, and forms molecular additive compounds with amino- and hydroxyl acids, carbohydrates, nucleotides, and vitamins through electron donor-acceptor interactions.

2.2 CARBORANES

Polyhedral heteroboranes have been a subject of intense research for over 50 years. A subset of this extensive class of compounds are dicarbadodecaboranes expressed by the general formula $C_2B_{10}H_{12}$.[1,2] Carboranes are a category of boron cluster compounds most widely explored in medicinal chemistry; however, other boron clusters, such as dodecaborate anion and boron cluster-based coordination compounds with boron clusters of different size (metallaboranes and metallacarboranes), also focus on growing attention.

Carboranes such as icosahedral dicarba-*closo*-dodecacarboranes ($C_2B_{10}H_{12}$) are characterized by rigid geometry, high chemical and biological stability, and an exceptional hydrophobic character. These characteristics support their use in designs based on the hydrophobic nature of carboranes. Metallacarboranes offer opportunities

related to the properties of metals being a part of the complex as well as unique structural features of the metallacarboranes molecule as whole.[3,4] Metallacarboranes comprise a vast family of metallocene-type complexes consisting of carborane cage ligands and one or more metal atoms such as Co, Fe, Cr, Nb, Ni, Cu, Au, Pt, Ru, Re,Tc, and many others. Application of metallacarboranes as vehicles for metals for modification of biomolecules is still underexplored.

An additional advantage of boron clusters and their metal complexes is that they are abiotic and therefore chemically and biologically orthogonal to native cellular components (stable biological environment) and usually resistant to catabolism, which is a desirable property of biological applications.

2.1.1 Structural features of carboranes

Polyhedral carborane clusters are characterized by delocalized electron-deficient linkages, meaning that there are too few valence electrons for bonding to be described exclusively in terms of 2-center-2-electron bonds. One characteristic of electron-deficient structures is the aggregation of atoms to form 3-center-2-electron bonds, which typically results in the formation of trigonal facets and hypercoordination. The high connectivity of atoms in a cluster compensates for the relatively low electron density in skeletal bonds. The three-dimensional deltahedral shapes are typical of boron and carborane cluster.

One of the best known types of polyhedral boron compounds are icosahedral dicarbododecaboranes ($C_2B_{10}H_{12}$) in which two BH vertices have been replaced by two CH units. They have nearly spherical geometry with 20 sides and 12 vertices, in which the carbon and boron atoms are hexacoordinated and participate in the heavily delocalized bonding. This, together with undergoing reactions typical for aromatic compounds, leads to the carborane molecule being characterized as a “pseudoaromatic” system. It is remarkable that the aromatic character of carboranes is expressed in three dimensions in contrast to two-dimensional aromaticity in planar polygonal hydrocarbons such as benzene.[1] The space occupied by dicarbadodecaborane is about 50% larger than that of the rotating phenyl group. Dicarba-*closo*-dodecaboranes (1,X-$C_2B_{10}H_{12}$) exist in three isomeric forms depending on the location of two carbon atoms within the cage, with X = 2, 7, 12, as *ortho*-, *meta*-, *para*-carboranes, respectively.

One of the most important features of a carborane system is its ability to enter into substitution reactions at both the carbon and boron atoms without degradation of

the carborane cage. The susceptibility for the removal of the most electrophilic boron atom is close-cage carborane such as 1,2-dicarba-*closo*-dodecaborane is an added advantage for its transformation into open cage form 7,8-dicarba-*nido*-undecaborate ion $(C_2B_9H_{12})^{-1}$, followed by the ability to form sandwich type derivatives which are analogs of the transition metal cyclopentadienide derivatives.

HYDROPHOBICITY OF CARBORANES

Carboranes and numerous metallacarboranes are characterized by exceptional lipophilicity or amphiphilicity. These properties make them particularly suitable for use as hydrophobic components in biologically active molecules, particularly those which interact hydrophobically with molecular targets in the cellular environment. The high hydrophobicity of many boron clusters and their derivatives can be explained by the presence of partial negative charge (density differs for different hydrogens and depends on the type of cluster), located on boron-bound hydrogen atoms in B-H group and their "hydrid-like" character. This prevents them from forming classical hydrogen bonds, which causes a lipophilic/hydrophobic character of the boron clusters.

The electronegativity of hydrogens enables boranes to form unconventional hydrogen bonds, namely dihydrogen bonds. Dihydrogen bonds, also called proton-hydride bonds, generally occur between a positively charged hydrogen atom of a proton donor *A*H (*A* = N, O, S, C, halogen) and a bond of an *M*H proton acceptor (*M* = electropositive atoms, such as boron, alkali metal or transition metal).[5] However, the dihydrogen bonds are weaker than classical hydrogen bonds; therefore, repulsive effect toward surrounding water molecules prevails, and the hydrophobic nature of many boron clusters observed. In boranes, NH···HB, CH···HB, and SH···HB dihydrogen bonds have been found. Another type of interaction was found for CH (carborane)-Y hydrogen-bonded complexes.

Boron clusters offer rich possibilities of tailoring the hydrophobic properties due to different dipole moments and hydrogen-binding sites of the molecule though there is only limited knowledge as to how to reach this in a geometrically predefined manner. The hydrophobicity of dicarbadodecaboranes can be reduced by the presence of a dipole moment, which is strongly dependent on the position of the carbon atoms in the carborane cluster. The hydrophobicity of dicarbadodecaborane isomers increases in the following order: 1,2-dicarba-*closo*-dodecaborane (*ortho* carborane) < 1,7-dicarba-*closo*-dodecaborane (*meta*-carborane), 1,12-dicarba-*closo*-dodecaborane (*para*-carbo-rane).

Removal of the most electrophilic boron atom in hydrophobic, neutral *closo*-carborane results in the formation of more hydrophilic, anionic *nido*-carboranes ($C_2B_9H_{12}^-$).

2.1.2 Applications of carboranes

The most important technical application of metallacarboranes is their utilization as selective extraction agents for lanthanide and actinide cations from nuclear waste solutions.[6,7] In the field of medicinal chemistry, boron cluster derivatives are used as high boron-content agents for boron neutron capture therapy (BNCT) and boron neutron capture synovectomy (BNCS)[8,9], radioimaging or magnetic resonance imaging (MRI).[10,11] Boron cluster moiety can also serve as the pharmacophore (3D analogue of aromatic group), namely as inhibitors of enzyme activity HIV-1 protease[12], cyclooxygenase[13]or serine protease[14]. Metallacarboranes (namely cobalt bis(dicarbollide) derivatives) substituted by proper exoskeletal organic groups are specific inhibitors of HIV protease and also effective inhibitors of its variants resistant to clinical inhibitors. This medical application led to the intense study of metallacarborane compounds and also to research relating to this diploma thesis, therefore this topic is described more in following paragraphs.

Carboranes in biochemical applications

The cage-like, ball-shaped dicarbadodecarborane structure mimics well the dodecahedral volume created by rotation of the planar phenyl ring over 360°, but it is bigger and has a much more hydrophobic moiety. Its higher volume and surface area in comparison with phenyl ring may explain the high-efficacy interactions of carborane-containing biomolecules with hydrophobic domains of proteins such as receptors. These advantages were first exploited for modification of amino acids and peptides. L-*Ortho*-carboranylalanine and several other carborane-modified amino acids were synthesized in the late seventies. The lipophilicity of L-*ortho*-carboranylalanine assigned by partition coefficient measurement was much higher than that of parent L-phenylalanine and higher than that of another lipophilic phenylalanine analog, L-adamantylalanine. Subsequently, several analogs of biologically active peptides have been synthesized. The recent revival of interest in the application of boron clusters in drug design associates on a range of receptor modulators containing carboranes as a hydrophobic pharmacophore, such as analogs of retinoic acid, estradiol, or androgene.

CARBORANE CLUSTERS AS HIV PROTEASE INHIBITORS

The aspartic protease of the human immunodeficiency virus (HIV) is one of the most extensively studied enzymes known to man. The HIV protease is crucial for the production of infectious viral particles,[15] and HIV protease inhibitors are potent and specific anti HIV drugs. The successful rational design of HIV protease is one of the most striking examples of structure-based drug design.

The discovery of metal bis(dicarbollides) as specific and potent inhibitors of HIV protease opens a new, unexpected pathway to the design of antivirals. It was found that some types of caboranes fit into the protease binding cleft, are biologically stable, and are enable facile chemical modification. After screening a number of structural motifs, icosahedral boranes and carboranes, namely metal bis(dicarbollides), were identified as promising frameworks for a novel class of non-peptide protease inhibitors.[12, 16] Main attention has been focused on ionic metal bis(dicarbollides).

The crystal structure of cobalt bis(dicarbollide) complexed to HIV protease showed that two cobaltacarborane cages are needed for efficient binding into the HIV-1 protease active-site cleft[12]. Therefore, the two parental cages were connected with a hydrophilic linker in order to increase binding affinity to the protease. N-substituted bis(ethyleneglycol) amine linker was used and it enables to modify the substitution pattern of the central part. Connecting the two clusters led to an improvement of inhibition in comparison with single cluster cobaltacarborane. These double-cluster compounds are easily synthetically accessible.

Biochemical studies revealed various modes of inhibition for various compounds. The competitive mode of inhibition implies that the inhibitor competes with the substrate for binding to the enzyme active site and this was, indeed, confirmed by two protein-ligand complex structures. The other inhibitory modes, mixed and non-competitive, suggest specific binding of compounds outside the enzyme active site or might also be explained by the activity of inhibitor aggregates that bind outside of the enzyme active site cavity.

Clearly, much remains to be learned before such compounds can be considered as tools for the treatment of humans; specifically, the aggregation of cobalt bis(dicarbollides) in aqueous solution seems to be a serious problem for the development of these compounds as potential drugs.

2.1.4 AGGREGATION OF METALLACARBORANES

Each anion of cobalt bis(dicarbollide) consists of two nido clusters, the surface of which is composed of nine hydridic hydrogen atoms that cannot form classical hydrogen bonds and two positively charged hydrogen atoms attached to carbon atoms. Since the overall negative charge is delocalized, cobalt bis(dicarbollides) exhibit superacidity and their salts are fully dissociated in water. All these attributes lead to a peculiar behavior of cobalt bis(dicarbollides) in aqueous media: the presence of delocalized negative charge and free-moving counterions manifests itself in a distinct amphiphilic character despite the lack of amphiphilic topology. The amphiphilicity is closely related to the surface activity. The detailed analysis of the self-assembly of cobaltacarboranes in aqueous solutions was provided recently,[17] forty years after the discovery of cobalt bis(dicarbollides) by Hawthorne. In aqueous solutions of sodium cobalt bis(1,2-dicarbollide), large aggregates with radii of approx. 100 nm were observed by light scattering and microscopy techniques.[17] The important fact is that the radius of the nanoparticles substantially varies with concentration, ionic strength and the aging of solution. Nevertheless, an inner structure of such huge nanoparticles is still unexplored.

The fact that the metallacarborane aggregates can be interpreted as rather temporal fluctuations of small subunits is partly supported by quantum mechanics calculations, which suggest that a mutual attraction of metallacarborane anions in the implicit solvent model is relatively weak and it only slightly beats a contribution of electrostatic repulsion.[18] Exoskeletal substitution of metallacarboranes leads to a complex aggregation behavior in aqueous solutions. Although the measure of hydrophobicity of boron cluster conjugates (e.g., the water-octanol partition coefficient) correlates fairly well with the association tendency in the solution,[19] a capability to aggregate is often controlled by electrostatic or other specific interactions among the linker, metallacarborane anion and its counterion. For example, a presence of highly charged groups like ATP attached to cobalt bis(dicarbollide) decreases its tendency to aggregate[19]. On the contrary, any aminofunctionalities, which can be protonated, form sparingly soluble zwitterions with metallacarboranes and the aggregation is pronounced in these cases.[19, 20] Fluorescence studies of two types of fluorescein-metallacarborane conjugates[21] revealed the cobalt bis(dicarbollides) can form large and ill-defined aggregates in water almost regardless of the nature of exoskeletal substituents. To increase solubility of the sparingly soluble metallacarborane conjugates and prevent the aggregation, extensive studies on the interaction of cobalt bis(dicarbollides) with

various biocompatible amphiphilic systems are strongly needed. In recent years, various studies dealing with the interaction of cobalt bis(dicarbollides) with cyclodextrins,[22,23] phospholipid bilayers,[21] surfactants[19,23] and hydrophilic polymers[18,23] have been published.

Interesting drug delivery system was prepared in form of stable micelle-like nanoparticles of block copolymer PEO–PMA with sparingly soluble fluorescein-metallacarborane conjugate, GB179 (Fig. 1).[21] Due to the chemical structure (two metallacarborane moieties per GB179 molecule attached to fluorescein via diethyleneglycol linkers) the fluorescein part cannot lose protons even in alkaline buffers. The probe is sparingly soluble and large pre-aggregates can be detected in aqueous solutions. After addition of PEO–PMA copolymer, the PEO blocks interact with the probe molecules. The copolymer chains penetrate by the PEO ends into the GB179 pre-aggregates, but the nanoparticles have to reorganize due to the bulkiness of GB179 at certain copolymer concentration reminding the critical micellar concentration. The nanoparticles are spherical and compact with well-pronounced core/shell architecture. The PEO blocks are considerably immobilized within the micellar core. The fraction of frozen PEO (ca. 50 %) is however smaller than in the case of micelles containing the parent cobalt bis(dicarbollide) (75 %).[18] This is due to the lower weight fraction, higher charge and bulkiness of GB179 within the micelles. The nanoparticles contain one GB179 molecule per roughly 150 PEO segments.

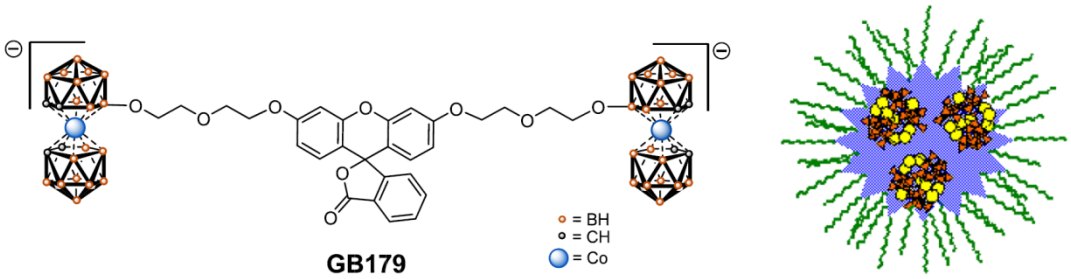

Figure 1 Chemical structure of GB179 and proposed structure of PEO–PMA/GB179 micelles in alkaline buffer. Color coding for metallacarborane: orange, boron; black, carbon; cyan, cobalt; hydrogen. Color coding for nanoparticle: green, polymeric chain; red, carborane moiety; yellow, fluorescein moiety.[21]

Another interesting example of carborane conjugate nanoparticles is nucleosides substituted by boron clusters in aqueous media. The combined LS and AFM study

revealed an intricate balance between hydrophobic and hydrophilic interactions and the sensitivity of the behavior to the nature of boron clusters: nucleosides with attached electroneutral or bulky charged clusters aggregate spontaneously, whereas nucleosides containing smaller and charged *nido*-clusters as well as the unmodified nucleosides remain in the form of true solutions or oligomolecular associates that are not observable by LS. The aggregation is strongly enhanced by the presence of amino groups because of the formation of zwitterions, which are sparingly soluble in the aqueous solution.[19]

PEO/ COBALT BIS(DICARBOLLIDE) COMPOSITE

It was found that poly(ethylene oxide) PEO interacts with cobalt bis(dicarbollide) and forms the insoluble composite, which can be exploited for preparation of polymeric nanoparticles.[18] The insoluble PEO/cobaltacarborane complex is deeply red colored, sticky, and hygroscopic matter. PEO displays a synergetic effect in the extraction of alkaline earth cations with metal bis(dicarbollide) anions into organic solvents.[24] The effect is explained by an interaction of metal cation with PEO units (confirmed also by crystallography),[25,26] which "increases" its solubility in organic media. Boron clusters also interact with polymer chains in water. Hence, the complex formation proceeds as a solubilization of cobalt bis(dicarbollide) anion in collapsing polymer coils. Significant contribution comes from an electrostatic attraction of bulky and amphiphilic double-cluster ions by cations complexed by PEO chains. These assumptions are in agreement with works on complexation of Na^+ with $-CH_2-CH_2-O-$ linkers covalently bound to boron clusters[27] and position of carborane counterions in protein structures.[28]

Quantum mechanics calculations showed that boron clusters interact with PEO repeating units via several noncovalent bonds between partially negatively charged hydrogen atoms attached to boron atoms in carborane cluster and partially positively charged H atoms in CH_2 units of PEO (Figure 3). Besides the formation of dihydrogen bonds, it is also important that cations interact with oxygen atoms of PEO. Hence, the salt concentration is the key factor which can be used for controlling the release in the drug delivery process.

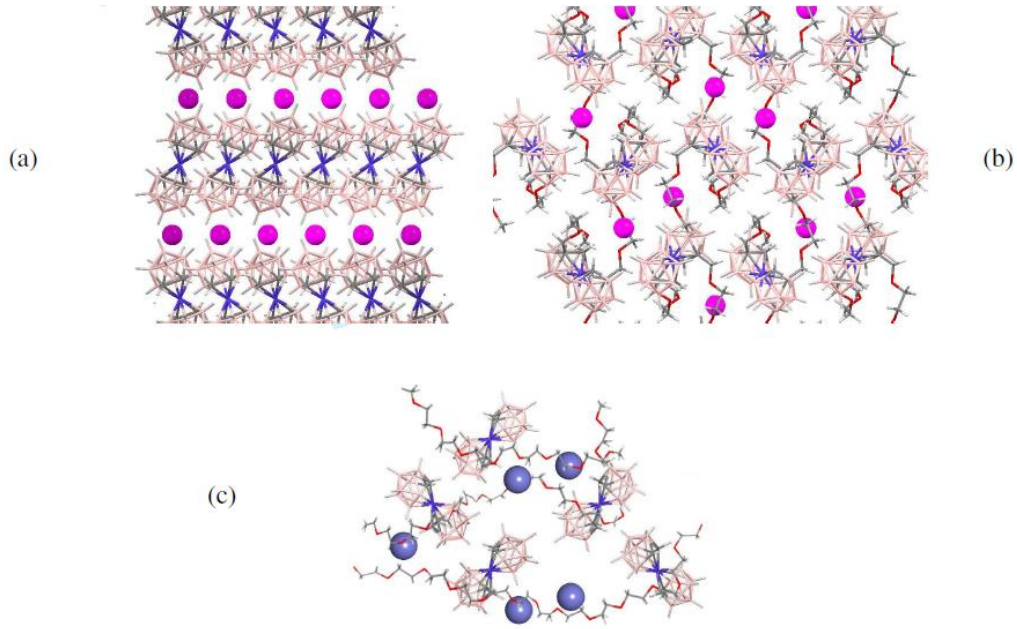

Figure 2 (a) $Cs[Co(1,2\text{-}C_2B_9H_{11})_2]$ and (b) $Cs[Co(1\text{-}CH_2OCH_2CH_2OCH_3\text{-}1,2\text{-}C_2B_9H_{10})_2]$ structures based on literature data (Refs. 57 and 69, respectively), and (c) the proposed structure of PEO/NaCoD composite; color coding: B salmon, C gray, O red, H white, Co Blue, Cs pink balls, Na blue balls.[29]

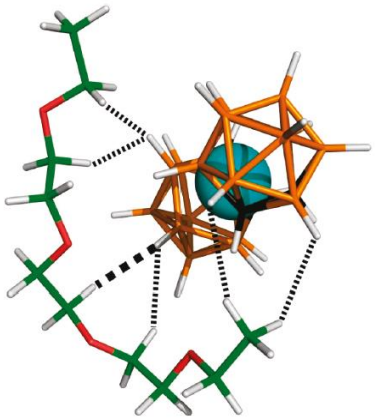

Figure 3 Optimized structure of the metallacarborane and PEO pentamer complex as a result of quantum mechanics calculations. Possible interactions are depicted. Color coding for metallacarborane: orange, boron; black, carbon; cyan, cobalt; white, hydrogen. Color coding for PEO pentamer: green, carbon; red, oxygen; white, hydrogen.[18]

2.3 COPOLYMERS

2.3.1 BLOCK COPOLYMER AND SELF-ASSEMBLY

Block copolymers are generally defined as macromolecules with linear and/or radial arrangement of two or more different blocks of varying monomer composition. In the last decade, the synthesis techniques have been widely extended, and especially ionic and controlled free radical methods can now be employed to prepare block copolymers with well-defined compositions, molecular weights and structures of very elaborate architectures. The increasing interest in block copolymers arises mainly from their unique solution and associative properties as a consequence of their molecular structure. In particular their surfactive and selfassociative characteristics leading to micellar systems are directly related to their segmental incompatibility. Thus micellization of block copolymers in a selective solvent of one of the blocks is a typical aspect of their colloidal properties. In fact when a block copolymer is dissolved in a liquid that is a thermodynamical good solvent for one block and a precipitant for the other, the copolymer chains may associate reversibly to form micellar aggregates. The micelles consist of a more or less swollen core of the insoluble blocks surrounded by a flexible fringe of soluble blocks. These micelles are generally spherical with narrow size distribution but may change in shape and size distribution under certain conditions. Block copolymers provide various application possibilities, such as colloidal assemblies as stabilizers, flocculants, nanoreservoirs, controlled drug delivery, gene therapy, phase transfer catalysis, surface modification, metal nanoparticles, latex agglomeration, stabilization of non-aqueous emulsions, etc.

2.3.2 AGGREGATION OF DIHYDROPHYLIC DIBLOCK COPOLYMERS

A particular class of water-soluble macromolecules, double-hydrophilic diblock copolymers (DHBCs, polymers with only hydrophilic but no hydrophobic blocks), has attracted great attention.[30] DHBCs have been intensely studied as stimuli-responsive materials.[31,32] and for their role in mineralization control of inorganic compounds.[33] Although DHBCs are an interesting class of materials, virtually no data on the behavior of pure DHBCs in aqueous solution exist. It is assumed in the literature that, unless triggered with an appropriate chemical (pH, ionic strength, complexation), physical (temperature, electric and magnetic field) or biochemical (enzymes, ligands) stimulus, these copolymers exist in dilute solution as single molecules in a random coil

conformation.[34] In spite of this, a few reports state that some DHBCs aggregate in pure water. Several independent studies have described the aggregation of poly(ethylene oxide)-*block*-poly-(N-isopropylacrylamide) (PEO-b-PNIPAM) and poly(N-isopropylacrylamide)-*graft*-poly(ethylene oxide) (PNIPAM-g-PEO) copolymers even below the lower critical solution temperature (LCST) of PNIPAM in water.[35-36] Attempts to explain this behavior include the suggestion by Berlinova et al.[36,37] that, as PNIPAM is quite hydrophobic at ambient temperature, it forms hydrophobic domains stabilized by the more hydrophilic PEO blocks forming micelle-like structures.

Recently the behavior of water-soluble poly(ethylene oxide)-*block*-poly(2-methyl-2-oxazoline) PEO−PMOX in aqueous solution was studied. Water solution contained small aggregates detected by DLS and PFG-NMR revealed an equilibrium between single chains and aggregates where the aggregate fraction is below 2% and the aggregate concentration was very low. PEO and PMOX, are water-soluble, but they are chemically different. These blocks have a significantly different capability for interaction with water. This can lead to a strongly preferred water uptake by one of the blocks, leading to a water gradient in the resulting aggregates and thus incompatible blocks.[38]

2.3.3 BRANCHED POLYMERS AND DENDRIMERS

Over the past decade, a great number of studies on dendrimers, hyperbranched polymer, and star-polymers have been published and they are rich area for new and unusual properties. The simplest branched materials are called star polymers in which several linear polymer chains are attached to only one branching point (core). These polymers contains chemically same or different arms (miktoarm star polymer) linked to the core. Star-block copolymers that all the arms consist of block or triblock copolymers have also been presented. Several methods have been utilized for the synthesis of star polymers.

One of the most important features of dendritic macromolecules is that the viscosity in solution and in melt is lower than their linear analogs. The viscosity of hyperbranched polymers depends on the degree of branching. Polymers have a variable hydrodynamic radii depending on the property of solvents. Hydrodynamic radii of hyperbranched polymers are smaller than those of their linear analogs with the same molar mass.

Various indirect experiments and molecular simulations indicate that the shape of dendrimers change from extended, open, structure to a spherical, densely packed structure, depending on the generation. Recently dendritic macromolecules with shape-persistent properties and rod shaped, cylindrical structures have been synthesized with several aims.

Specific amphiphilic star copolymers synthesized by Gitsov and Fréchet[39] are able to change their conformation depending on the environment.[40] The star copolymers can form monomolecular micelles with different core-shell structure as a function of the environment. It is suggested that these stimuli-responsive macromolecules might be useful as delivery vehicles of encapsulation and release of hydrophobic or hydrophilic species.

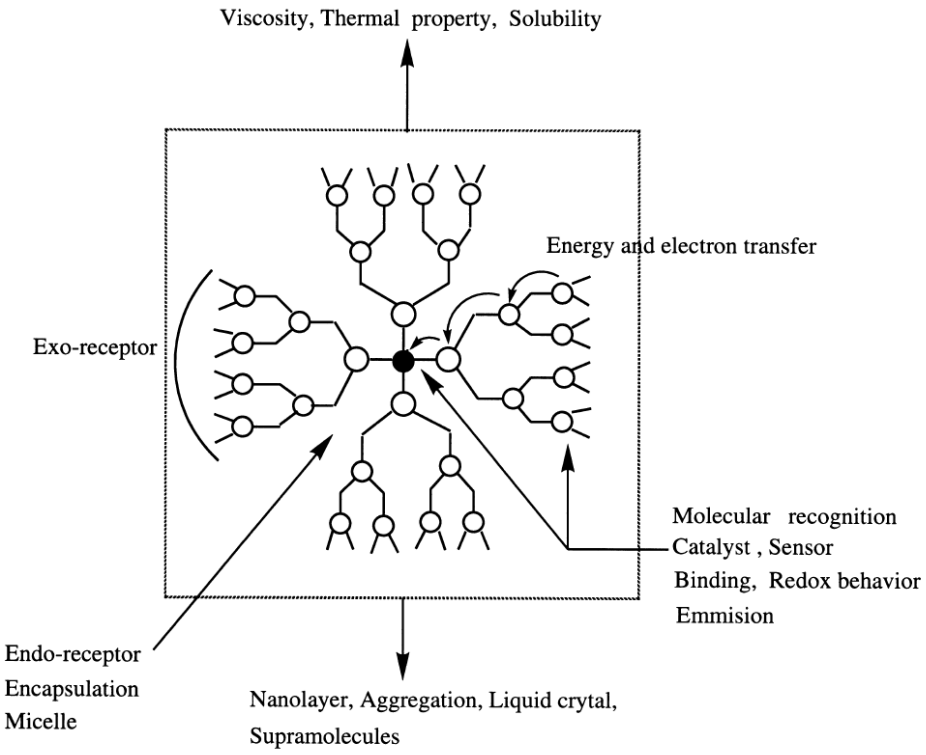

Figure 4 Schematic representation of properties of dendrimers and their potentials as functional macromolecules.[41]

One of the most useful applications of dendritic structures is in the area that multifunctional groups in ordered array are required. Three-dimensional chiral dendrimers containing chiral units in the interior and/or on the surface have many features, which can offer the opportunity to meet functionalities such as high molecular recognition, chemical separation, and asymmetric catalysts. Considering future advanced materials, the combination of functional dendrimers and well-controlled linear

polymers might be useful tools for creating new functional materials made up for the defects of each component.

2.3.4 Poly(2-oxazoline)s

The cationic ring-opening polymerization of 2-oxazolines was discovered in the middle of the 1960s by four independent research groups.[42,43] Furthermore, the early possible applications of poly(2-oxazoline)s as stabilizers/surfactants, compatibilizers, and thermosettings were addressed by Kobayashi and Uyama.[8] In recent years, the use of poly(2-oxazoline)s in biomedical applications[44] has evolved as a result of their biocompatibility as well as their stealth behavior - suppression of all interactions with the body, such as with proteins and the immune system. Furthermore, the discovery that poly(2-ethyl-2-oxazoline) (PEOX) exhibits a lower critical solution temperature in water[45] opened up a completely new research area on thermoresponsive materials. Furthermore, the easy access to hydrophilic, hydrophobic, and fluorophilic polymers by simply changing the side chain of the monomer stimulated investigations into the synthesis and self-assembly of a range of amphiphilic copolymer structures. Unambiguous proof of the biocompatibility and stealth behavior of poly(2-methyl-2-oxazoline) (PMOX) and poly(2-ethyl-2-oxazoline) (PEOX) decorated liposomes was provided by Zalipsky and coworkers.[46] The biocompatibility, stealth behavior, and biodistribution of PMOX closely resemble the beneficial properties of PEO that boosted its widespread use in biomedical applications. It should be noted that PMOX is more hydrophilic than either PEOX or PEO,[47] which might complicate conjugation reactions in apolar organic solvents. Nonetheless, PMOX has great potential for use in biomedical applications, although in-depth studies have to be performed to further evaluate the fate and possible degradation pathways when used in vivo. The potential formation of poly(ethylene imine) residues by enzymatic degradation of the amide bonds of poly(2-oxazoline)s[48] have to be studied in detail in particular, since copolymers of 2-ethyl-2-oxazoline and ethylene imine are known to exhibit higher cytotoxicity than PEOX.[49]

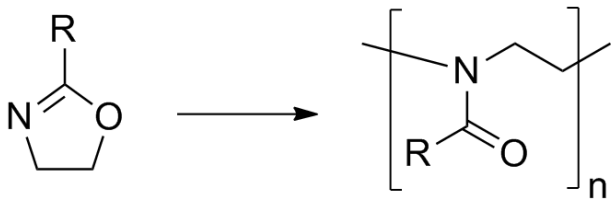

Scheme 4 Polymerization of 2-oxazolines.

2.4 Interactions of counterions with carboranes and polymers

Cations in aqueous solution interact with both metallacarboranes and polymeric chains. As it was described in Section 2.1.4, the formation of multimolecular associates of cobalt bis(dicarbollide) is a complex process that can be influenced by concentration of cations among others. The exact structure of the aggregates is still unknown, but it is obvious that counterions should play an important role. Interaction with counterions is also closely related to the application in the field of extraction chemistry. Interactions of cations with polymers have been studied mostly for PEO and alkali and alkaline-earth metal salts.

2.4.1 Carboranes in extraction

A characteristic feature of cobalt bis(dicarbollide) anion is good solubility of its free conjugated acids and most of their salts in medium-polarity solvents such as ethers, nitrosolvents, halogenated solvents, and so on, to which they can be extracted from the water phase together with alkali metal cations. The unique importance cobalt bis(dicarbollide) anion in the design of extraction agents lies in the extraordinary chemical and thermal stability due to "pseudoaromaticity" and to the completely filled electronic shell of the Co(III) cation that is furthermore sterically shielded by two bulky dicarbollide ligands. The central cobalt atom thus behaves as chemically inert and stable toward a nucleophilic attack.

In 1970s it was found that cobalt bis(dicarbollide) anion is suitable agent for extraction of biotoxic ^{137}Cs from spent nuclear fuel, which was important for both economic and ecological reasons. The basic chemistry of this extraction involves the transfer of the dissociated ion pair consisting Cs^+ cation with cobalt bis(dicarbollide) anion from the water phase to the nitrobenzene phase. No chemical reaction or complexation occurs and only hydration and solvation forces apply. At first sight, the high extractability of Cs^+ ion into nitrobenzene could be connected with special affinity of this organic solvent toward Cs^+. However, this is not the case. Indeed, Cs^+ is much less solvated by nitrobenzene than by water, and the extraction is in fact facilitated by the extremely affinity of the ion pair toward nitrobenzene. From the acidic media, Cs^+ is extracted due to rather high extraction-exchange constant $K(Cs^+/H^+)$ because H^+ is still much less solvated than bis(dicarbollide) anion. Some less hydrophobic cations such as Sr^+ or Eu^{3+} can be made more hydrophobic by complexing them with various ligands.

2.4.2 COUNTERIONS AND POLY(ETHYLENE OXIDE)

Ionic conducting polymers comprised of PEO oligomers complexed with different alkali- and alkaline-earth metal salts of weakly coordinating anions are of considerable interest. These solid polymer electrolytes find a wide variety of their potential applications in high-energy density batteries and electrochromic devices.[50] The solvation of salts, for example, $LiCF_3SO_3$ [3] or $Li(CF_3SO_2)_2N$ [4,5] in PEO oligomers, represented by $H_3CO(CH_2CH_2O)nCH_3$, exhibit significant ionic conductivity[50] partly attributed to the cation–anion or cation–polymer interactions and the polymer segment motion. The metal ion (alkali, alkaline or lanthanides) coordinated to ether oxygens of PEO oligomers engenders solubilization of a salt forming a polymer–salt complex. These metal ion–oxygen interactions influence the local structure of a polymer backbone[51] and can be studied by measuring the infrared and Raman spectra.

Dhumal et al. theoretically studied metal ion-PEO oligomer represented by M-$CH_3O(CH_2CH_2O)_nCH_3$ (n = 2–7) (M = Na^+, K^+, Mg^{2+} and Ca^{2+}) by employing the *ab initio* and hybrid density functional methods.[52] The metal ions bind strongly to the ether oxygens of PEO oligomers. This results in the weakening of the CO bonds. Calculations also showed that the intensity of CO stretching vibrations in 1:1 ion-pair complex of $CH_3O(CH_2CH_2O)_nCH_3$ (n = 2–7) is decreasing as follows: $K^+ > Na^+ > Ca^{2+} > Mg^{2+}$, which is consistent with the predicted binding energies of ion-pairs of tri- to hepta-glymes, which increases from K^+ to Mg^{2+}.

Charged-induced conformational changes of poly(ethylene oxide)-sodium system (PEO-$(Na^+)_n$) in a vacuum and water droplets were studied using molecular simulations by Consta et al.[53] They investigated solvation effects of the charged PEO by simulating PEO96-$(Na^+)_4$ system in nanosized droplets of water and also a neutral PEO in the same droplet. They found that in both cases, it stays in a uniformly extended conformation. The effect of sodium ions (and possibly extra ions present) was that the neutral PEO stayed in the interior of the water droplet, while the charged PEO (with or without extra sodium ions) stayed close to the surface. The behavior of the neutral PEO could be explained by its well-known hydrophilic nature. On the other hand, for the sodiated PEO, some of its hydrophilic oxygen atoms surround sodium ions, leaving hydrophobic ethylene groups exposed unfavorably to water. As a result, the whole molecule is expected to be pushed away from the interior of the water droplet.

Simulations of conformational transition showed that the smallest system of PEO_{54}-$(Na^+)_3$ showed frequent transition between a compact shape and a more extended

shape, although the extended one did not correspond to a local minimum of the free energy profile of the system as a function of a radius of gyration. Larger systems with longer PEO also showed the systematic trend of higher probability density for compact conformations.

3 MATERIAL, SAMPLE PREPARATION AND METHODS

3.1 MATERIAL

Metallacarborane sodium [3-cobalt bis(1,2-dicarbollide)]$^-$ Na[**1**] was a kind gift of Bohumír Grüner and Jaromír Plešek (Institute of Inorganic Chemistry, Academy of Science of the Czech Republic, Řež near Prague). For polymer titration experiments we used Cs[1], which was purchased from Katchem Ltd. (Czech Republic) and it was converted to Na[**1**] by extraction described by Plesek. [Plesek, J.; Base, K.; Mares, F.; Hanousek, F.; Stibr, B.; Hermanek, S. Collect. Czech. Chem. Commun. 1984, 49, 2776]. It has been characterized using mass spectrometry and ^{1}H and ^{11}B NMR spectroscopy and in aqueous solutions by other techniques. Metallacarborane conjugates GB42 (**2**), GB48 (**3**), GB80 (**4**), GB105 (**5**), GB124 (**6**) and GB225 (**7**) were prepared in form of sodium salts by Bohumír Grüner and designed as HIV protease inhibitors. Structures of metallacarborane inhibitors are shown in Scheme 1.

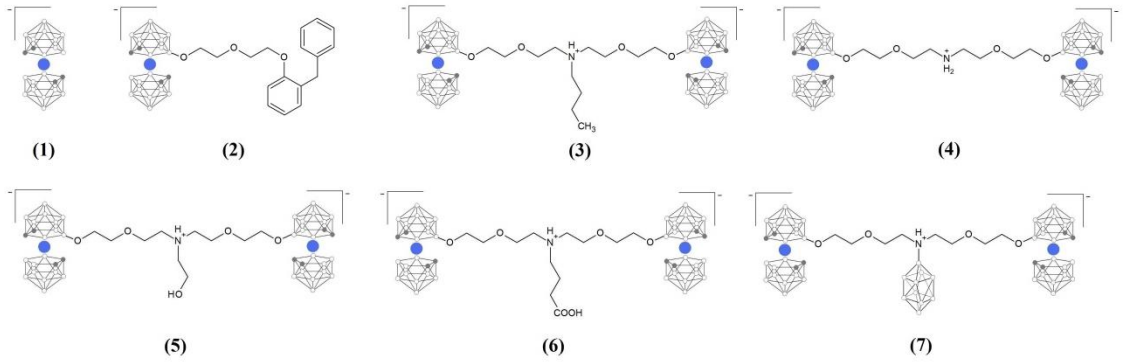

Scheme 1 Structures of metallacarborane inhibitors used in this study.

Other metallacarborane conjugates – dumbbells, were synthesized by Màrius Tarrés (Institut de Ciència de Materials de Barcelona). It has been characterized using mass spectrometry and ^{1}H and ^{11}B NMR spectroscopy. Metallacarborane dumbbells were prepared in form of different salts. The cations used for dumbbells are H^+, Li^+, Na^+, K^+ and NMe_4^+. Structures of all dumbbells are shown in Scheme 2. The concentration of saturated solutions was estimated from extinction coefficient determined for the sample Na_2[**8**] in water solution, ε(307nm) = 36,793 $M^{-1}cm^{-1}$ (band of cobalt bis(dicarbollide).

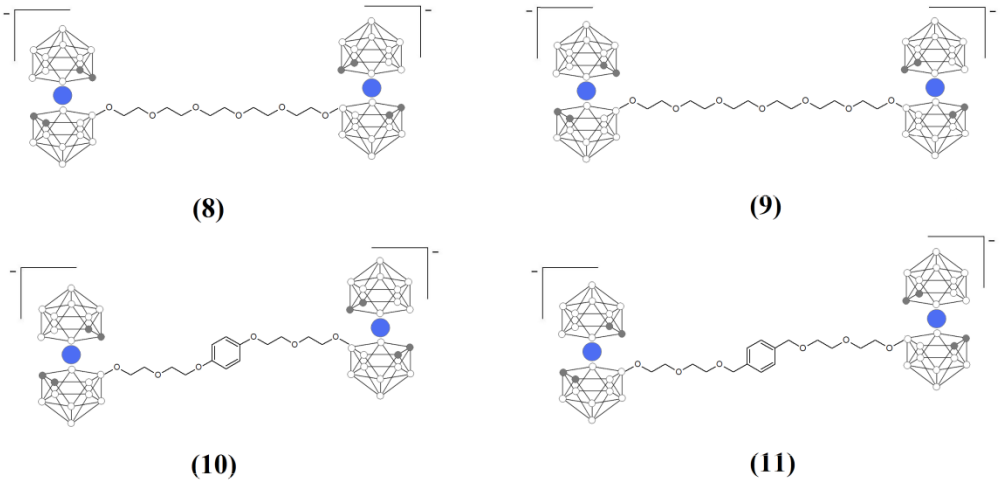

Scheme 2 Structures of metallacarborane derivatives (dumbbelles) used in this study.

All polymers used in this study were purchased from Polymer source, Inc. (Dorval, Quebec, Canada). The polymers used in this study are double-hydrophilic block copolymer poly(ethylene oxide)-*block*-poly(2-ethyl oxazoline), PEO-PEOX, triblock copolymer poly(2-ethyl oxazoline)-*block*-poly(ethylene oxide)-*block*-poly(2-ethyl oxazoline), PEOX-PEO-PEOX and star-like copolymer, 4-arm poly(ethylene oxide)-*block*- poly(2-methyl oxazoline), PEO-PMOX. The structures of all polymers are shown in Scheme 3. Their weight averaged relative molecular weight and dispersity is shown in Table 1.

(1)

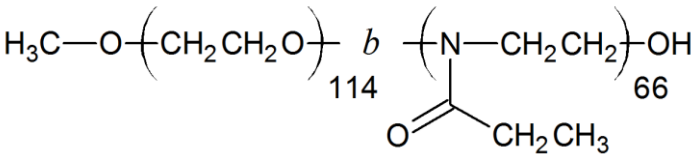

(2)

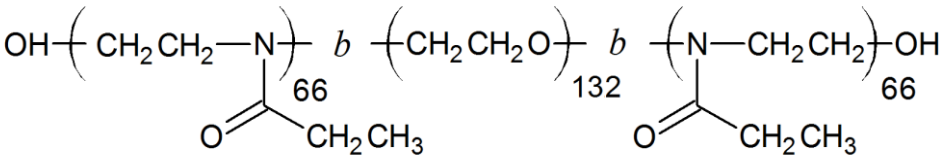

(3)

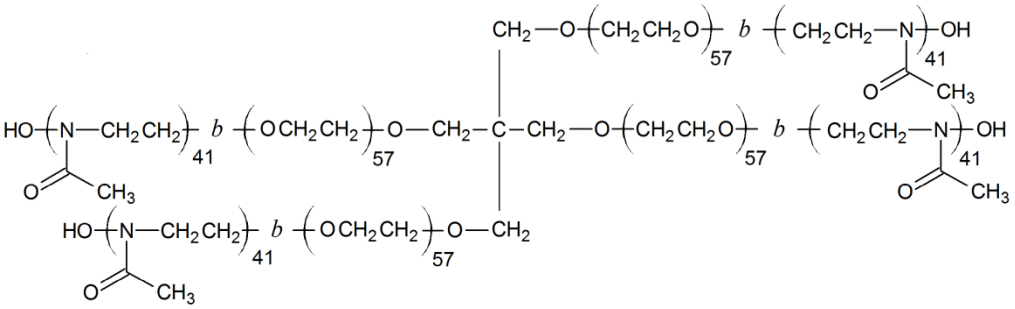

Scheme 3 Structures of all polymers used in this study as provided by the manufacturer: (1) poly(ethylene oxide)-*block*-poly(2-ethyl oxazoline), (2) poly(2-ethyl oxazoline)-*block*-poly(ethylene oxide)-*block*-poly(2-ethyl oxazoline) and (3) 4-arm poly(ethylene oxide)-*block*-poly(2-methyl oxazoline).

Table 1 Weight averaged relative molecular weight and dispersity of the polymers used in this study.

	M_w/M_n	M_n
PEO-PEOX	1.4	PEO (5000) – PEOX (6500)
PEOX-PEO-PEOX	1.4	PEOX (6500) – PEO (5800) – PEOX (6500)
4-arm PEO-PMOX	1.5	PEO (2500) – PMOX (3500)

3.2 SAMPLE PREPARATION

Dumbbells in water and salt solution

Saturated solutions of dumbbelles were prepared in deionized water and 0.154 M chloride of corresponding counterion and after stirring they were centrifugated (5 min, 12,000 rpm). The concentration of samples was estimated from absorbance. The presence of aggregates was monitored by light scattering.

Cobalt bis(dicarbollide) anion in solutions with polymers

The samples for SAXS study were prepared by quick addition of Na[**1**] solution in 0.1 M NaCl to 200 μL of PEO-PEOX solution (10 g/L) in 0.1 M NaCl.

The samples for NMR study were prepared by mixing of calculated amount of solid Na[**1**] with 2 mL of PEO-PEOX solution (10 g/L) in 0.00 M, 0.01M and 0.10 M NaCl in D_2O in order to obtain mixtures with **1**-to-polymer segment ratio $\xi = 0.015$ and 0.045. Small amount of *t*-butyl alcohol (*t*-BuOH) was added to the solutions as an

internal standard. We used polymer solutions with relatively high concentration of polymer for NMR to get signals of sufficient quality. As a smaller amount of solution is needed for NMR as compared to LS-titration, we did not add the metallacarborane solution consecutively but directly the appropriate portion of solid sample to the polymer solution in order to skip the unstable region (low content of metallacarborane).

The solutions of PEO-PEOX, PEOX-PEO-PEOX and 4-arm PEO-PMOX (c = 2 g/L, 5 mL) were consecutively titrated by Na[**1**]. Concentration of Na[**1**] was adjusted to get the same ratio n(seg)/n(cosan) for all three cases: for PEO-PEOX $c_{Na[1]}$ = 0,0242 M, for PEOX-PEO-PEOX $c_{Na[1]}$ = 0,0190 M and for 4-arm PEO-PMOX $c_{Na[1]}$ = 0,0251 M. The titration experiments with different salts were carried out as follows: Na[**1**] (c = 0.019 M) in 0.154M NaCl, LiCl or KCl respectively, was added to PEO-PEOX (2g/L) in 0.154M NaCl, LiCl and KCl solution respectively. All time lags were less than half an hour and the solutions during the titration process were analyzed by a measure of light scattering.

Conjugates of cobalt bis(dicarbollide) in solutions with polymers

In titration experiments with dumbbells stock salt solutions of polymer PEO-PEOX, PEOX-PEO-PEOX and 4-arm PEO-PMOX (20 g/L) were added to 3 mL of Na_2[**8**] and to 6 ml of Li_2[**8**] and K_2[**8**]. Solution of Na_2[**8**] was saturated (5.21×10^{-5} M), concentration of Li_2[**8**] was lower than saturated (4.0×10^{-4} M) because of high solubility (0.00313 M). Concentration of K_2[**8**] was higher than saturated (1 mg in 3 mL) because of low solubility of this sample (1.67×10^{-6} M). Time lag between each addition was less than an hour for Na_2[**8**] and Li_2[**8**]. In case of suspension of K_2[**8**], time lag was longer, about an hour. Polymer stock salt solutions were filtered through 0.45 μm Acrodisc filters. All solutions were prepared in corresponding 0.154 M salt solution: NaCl, LiCl or KCl and analyzed by light scattering.

In experiments with HIV protease inhibitors, 3 mg of GB42 (**2**), GB48 (**3**), GB80 (**4**), GB105 (**5**), GB124 (**6**) and GB225 (**7**) were mixed with 2 mL of water, physiological saline (0.154 M NaCl) with/without copolymer PEO-PEOX (10 g/L). All the mixtures were sonicated (30 min) and left to shake overnight. The metallacarborane content was obtained by measuring of UV/Vis of clear centrifugated solutions.

For absorbance and DLS measurements, dumbbells in polymer solutions were prepared by mixing 1 mg of solid dumbbell sample with 1 mL of 10 g/L of polymer in 0.154 M corresponding salt solution and they were left to shake overnight. After

centrifugation the solubility was estimated from absorbance and the presence of aggregates was monitored by light scattering.

3.3 METHODS

Dynamic Light Scattering (DLS) and Static Light Scattering (SLS). The light scattering setup (ALV, Langen, Germany) consisted of a 633 nm He-Ne laser, an ALV CGS/8F goniometer, an ALV High QE APD detector, and an ALV 5000/EPP multibit, multitau autocorrelator. DLS data analysis was performed by fitting the measured normalized intensity autocorrelation function $g_2(t) = 1 + \beta|g_1(t)|^2$, where $g_1(t)$ is the electric field correlation function, t is the lag-time and β is a factor accounting for deviation from the ideal correlation. An inverse Laplace transform of $g_1(t)$ with the aid of a constrained regularization algorithm (CONTIN) provides the distribution of relaxation times, $\tau A(\tau)$. Effective angle- and concentration-dependent hydrodynamic radii, $R_H(q,c)$, were obtained from the mean values of relaxation times, $\tau_m(q,c)$, of individual diffusive modes using the Stokes-Einstein equation. To obtain true hydrodynamic radii, the data have to be extrapolated to a zero scattering angle. Since the refractive index increment, dn/dc, is unknown for almost all of the samples, we evaluated in such cases only the light scattering intensity extrapolated to zero scattering angle as the measure proportional to molar mass of polymeric nanoparticles.

UV-Vis spectroscopy. UV-Vis absorption spectra were carried out with a Hewlett-Packard 8452a diode-array spectrometer.

Isothermal Titration Calorimetry (ITC). ITC measurements were performed with an Isothermal Titration Calorimeter (Nano ITC), TA Instruments - Waters LLC, New Castle, USA. The microcalorimeter consists of a reference cell and a sample cell (24K Gold). The sample cell is connected to a 100 (50) μL syringe. The syringe needle is equipped with a flattened, twisted paddle at the tip, which ensures continuous mixing of the solutions in the cell rotating at 200 (250) rpm. Titrations were carried out by consecutive 5 μL injections of 24.5 mM Na[**1**] in 0.00, 0.01 and 0.10 M NaCl aqueous solutions from the syringe into the sample cell filled with 960 (193) μL of 0.5 g/L PEO-PEOX and PEOX in 0.00, 0.01 and 0.10 M NaCl aqueous solution. A total of 20 injections were performed with intervals of 1800 s. These injections replace a part of the solution in the sample volume and the changed concentration is considered in the

calculation of the sample concentration. By this method then the differential heat of mixing is determined for discrete changes of composition. The data were analyzed using the NanoAnalyze software by fitting with a simple one-site binding model.

^{1}H NMR spectroscopy. ^{1}H NMR spectra were measured on a Varian $^{\text{UNITY}}$*INOVA* 400 in deuterium oxide (99.5 %; Chemotrade, Leipzig, Germany). Spectra were referenced to the solvent signal (4.80 ppm).

Small Angle X-ray Scattering (SAXS). SAXS experiments were performed using a pinhole camera (Molecular Metrology SAXS System) attached to a microfocused X-ray beam generator (Osmic MicroMax 002) operating at 45 kV and 0.66 mA (30 W). The camera was equipped with a multiwire gas-filled area, detector with an active area diameter of 20 cm (Gabriel design). Two experimental setups were used to cover the q range of 0.005 – 1.1 $Å^{-1}$ Scattering vector, q, is defined as: $q = (4\pi/\lambda)\sin\theta$, where λ is the wavelength and 2θ is the scattering angle. The scattering intensities were put on absolute scale using a glassy carbon standard.

4 RESULTS AND DISCUSSION

The first part of results and discussions is focused on the study of dumbbells – conjugates of two cobalt bis(dicarbollide)s in aqueous and salt solutions. The second part is focused on parent cobalt bis(dicarbollide) cluster in solution with block copolymers containing PEO and poly(2-alkyl oxazoline) blocks. The aim of the last part of results was characterization of solutions of the same polymers with cobalt bis(dicarbollide) conjugates: dumbbells (from the first part) and double-cluster compounds with HIV protease inhibition activity.

4.1 DUMBBELLS IN WATER AND SALT SOLUTION

4.1.1 SOLUBILITY IN AQUEOUS SOLUTIONS

The structures of the studied dumbbells compounds **8** – **11** are shown in Scheme 2. Saturated solutions of Na^+, Li^+, K^+, H^+ and NMe_4^+ salts of dumbbells were prepared in pure water and 0.154 M chloride of corresponding cation (except NMe_4^+ salt). From the UV-VIS measurements of absorbance, the solubility of solutions *S* was calculated (at wavelength 307 nm). From solubility of solutions the solubility product was calculated according the relation based on the metallacarborane structure: $K_{sp} = [A^+]^2 [B^{2-}] = 4S^3$, where A^+ and B^{2-} are corresponding cations and anions, respectively. In Figure 5 we can see differences in solubility described by pK_{sp}, which was calculated from the relation pK_{sp} = - logK_{sp}.

Sodium and lithium dumbbells are the most soluble with pK_{sp} 8.4 ± 2.9 and 7.3 ± 1.6, respectively. It seems that the nature of the handle influences the value of pK_{sp}. Increasing length of the PEG linker causes lower solubility of sample and it is also evident that the presence of *p*-phenylene subunits in linker affects solubility. Dihydroxybenzene group in the handle increases solubility, while dihydroxy-*p*-xylene group has the opposite effect.

The impact of the handle became smaller for hydrogen and potassium dumbbells. They are both sparingly soluble with pK_{sp} 11.2 ± 0.6 and 11.0 ± 0.8, respectively. Increasing length of the PEG chain in potassium dumbbells has the same tendency as for Na^+ and Li^+ samples, while the solubility of H^+ dumbbells stays almost

the same. The effect of *p*-phenylene subunits on the value of pK_{sp} is obvious for all dumbbells.

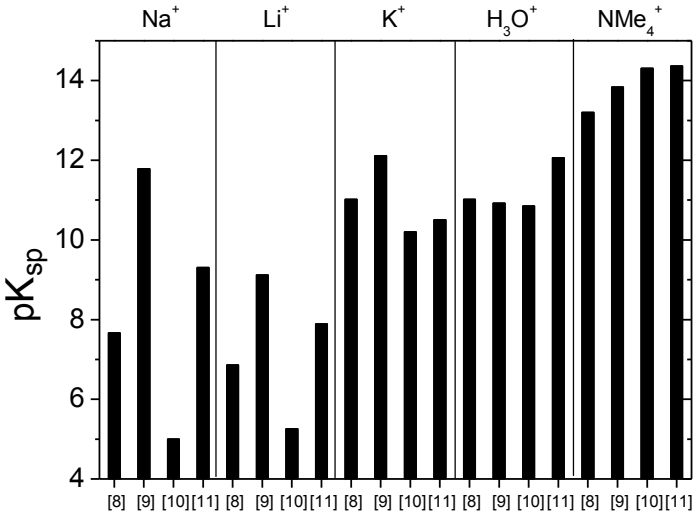

Figure 5 Solubility product of dumbbells samples.

NMe_4^+ salts are the most insoluble with pK_{sp} = 13.9 ± 0.5. An influence of the handle is very low. However we can still see the tendency of longer handle to decrease solubility of dumbbell sample.

In Figure 6 we can see the comparison of solubility of dumbbells in water and in salt (S_{salt} divided by S_{water}). The solubility of all the samples is lower in 0.154 M salt solutions. This is mainly due to the common ion effect. However there are also other influences as we can see from the differences among dumbbells. It is interesting that the impact of salt on sodium dumbbells is very variable, from 0.03% for Na_2[**10**] to 45% for Na_2[**9**]. Very broad range was also observed for LiCl solutions, from 0.2% for Li_2[**10**] to 97% for Li_2[**8**]. For potassium dumbbells the presence of salt led to the highest decrease of solubility, difference was less than 1.3%. For potassium samples only, we can see specific influence of *p*-phenylene subunits in the handle that leads to the lower solubility of KCl solutions as compared to those in pure water. Additional ITC measurements (data not shown) also showed that the affinity of K^+ to the PEG-handle is probably the highest among the studied alkaline cations, which reflects low solubility of potassium dumbbells. For dumbbell acids in HCl solution, the solubility dropped to less than 5% and the impact of handle seems to be negligible.

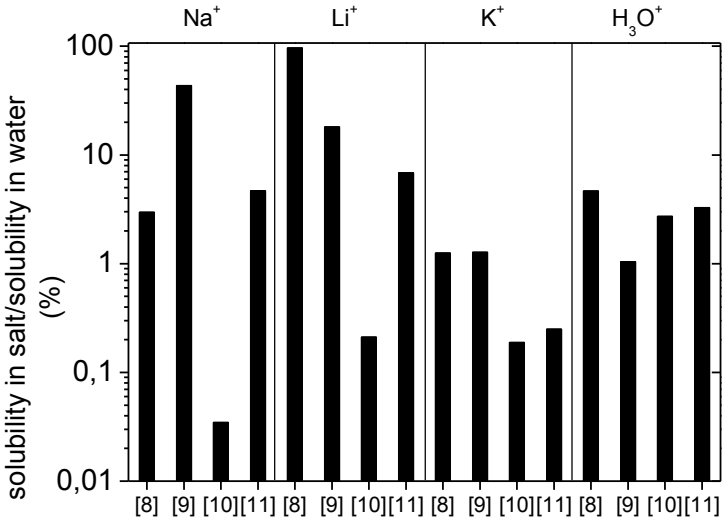

Figure 6 Solubility in salt relative to that in pure water in %.

The solubility differences are often very difficult to explain and predict. However we could distinguish some trends in above-described study of dumbbell molecules in water and salt solutions. Salts of **1** are often very water-soluble even though the metallacarborane cluster is hydrophobic. One of the main reasons is probably negative charge and the entropy of corresponding counter-ions. Therefore immobilization of cations can cause decrease of solubility. As it was mentioned in Section 2.4.2, Na^+, Li^+ and K^+ ions interact with PEG linker and this partial complexation plays significant role in forming of particles and solubility of solution. Difference in behavior of H_3O^+ dumbbells is probably caused by a direct interaction with clusters, or with very negative oxygen atoms bound to B8 atoms in dumbbell molecules. Hence, a chemical structure of the linker does not play such an important role as in the case of alkaline cations. The same is true for NMe_4 salts, which are sparingly soluble and the presence of the linker has almost no impact on solubility.

Generally, we can say that increasing length of PEG linker leads to decrease of solubility. *p*-phenylene subunits in the handle probably also influence complaxation of alkaline cations. Complexation of counterions is tightly related with even more complicated process – aggregation of metallacarborane in aqueous solutions.

4.1.2 Aggregation of dumbbells in aqueous solutions

According to well-known aggregation behavior of metallacarboranes (Section 2.1.4), DLS measurements of dumbbells samples in water and 0.154 M salt solutions were

carried out. Concentration dependences of dumbbell samples in water and salt solutions were examined (Figure 7, 8). All the solutions contained aggregates, and their distribution was mainly monomodal. As we can see in Figure 7 and 8, the size of aggregate varies with concentration and this process strongly depends on concentration of dumbbell sample. The increase of size of particles with decrease of concentration, which is observation typical for pure **1**, was confirmed only for some of the dumbbells samples. As the size of different dumbbell particles is variable for different content of carborane, we can say that the presence of the handle has the impact on aggregation. However the trends are not very clear and all R_H and scattering intensity dependences are complex and difficult to explain.

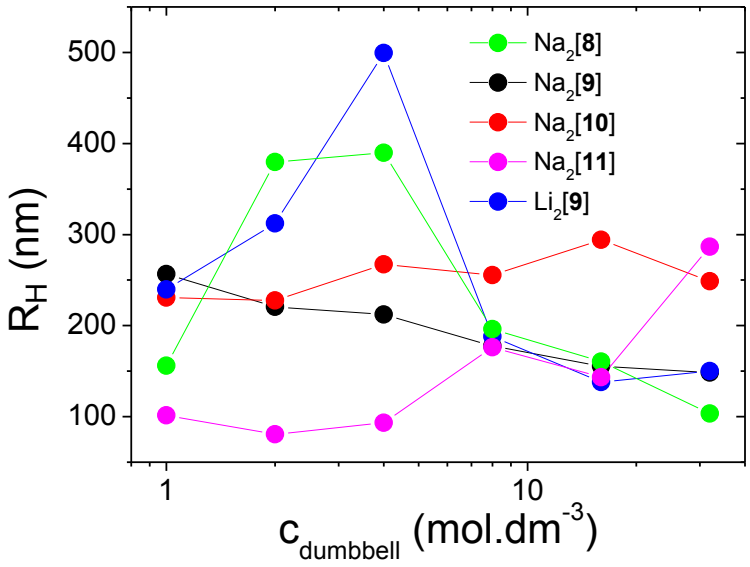

Figure 7 Concentration dependence of the size of dumbbell aggregates in pure water.

Worth-noticing is bimodal distribution of size of Na$_2$[**8**] particles at elevated concentrations in salt solutions. In water solutions only one type of particle was present with size in range of 100 - 400 nm. In salt solution one mode of large particles (200 - 400 nm) became bimodal for higher concentration of sodium dumbbell. Small 2-3 nm particles were detected coexisting with larger particles of size around 100 nm. Predominant fraction of small nanoparticles was also observed for lithium samples. This is for the first time such small nanoparticles were observed in the solution of metallacarboranes by DLS. These particles could be formed by only few molecules of carborane compound or even single dumbbell molecules, which are probably present in the solution. We suppose that they accompany larger particles even in other solutions

but their DLS-signal is weaker so they are not visible by DLS. In the region of higher concentration in salt solution, the large aggregates split into the small ones so their signal prevails.

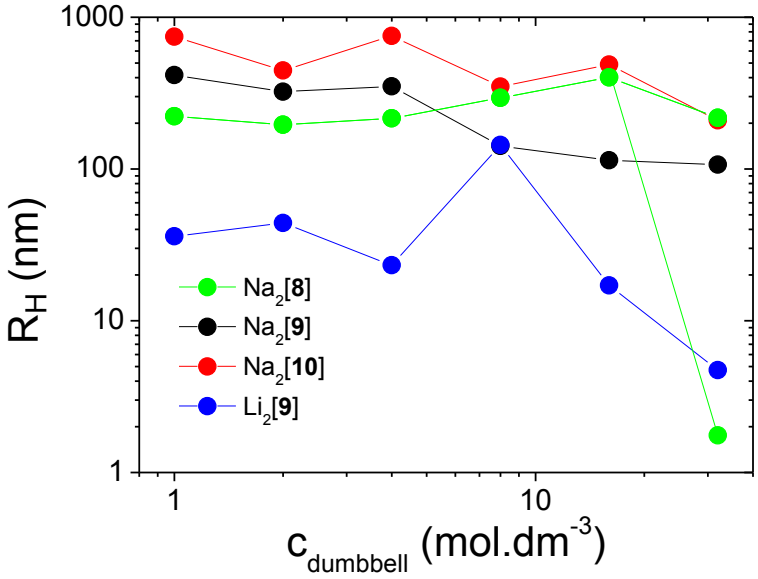

Figure 8 Concentration dependence of the size of dumbbell aggregates in salt solutions.

This trend is demonstrated by DLS distributions of hydrodynamic radii of Na_2[**8**] and Li_2[**8**] in Figure 9, where we can see one mode corresponding to the large particles in saturated solution of Na_2[**8**] in water. Saturated saline solution of Na_2[**8**] contained also second mode of small particles. As we can see, the fraction of 2nm particles is quite high. This interesting phenomenon has been observed also by cryoTEM imaging (not shown). Very unexpected result was observed in case of Li_2[**8**] salt solution, which contained only small 3 nm particles.

For the deeper study of influence of counterions on aggregation process and size of aggregates, DLS dependences of salt concentration on hydrodynamic radii were examined, the results are shown in Figure 10. The values of R_H vary with salt concentration but no trend was observed and results are again difficult to interpret. However we can see that the concentration of counterions is important variable in aggregation process and cations of salts are probably part of formed aggregates.

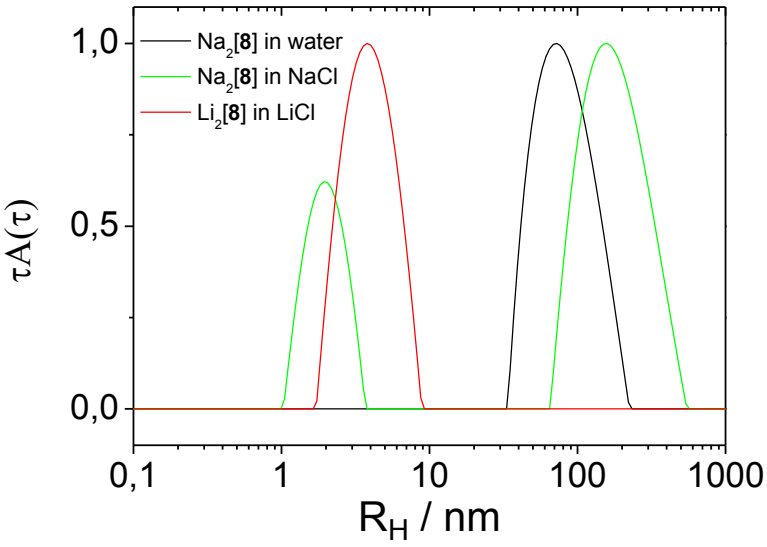

Figure 9 DLS distributions of saturated solution of Na_2[**8**] in pure water and 0.154 M NaCl and saturated solution of Li_2[**8**] in 0.154 M LiCl.

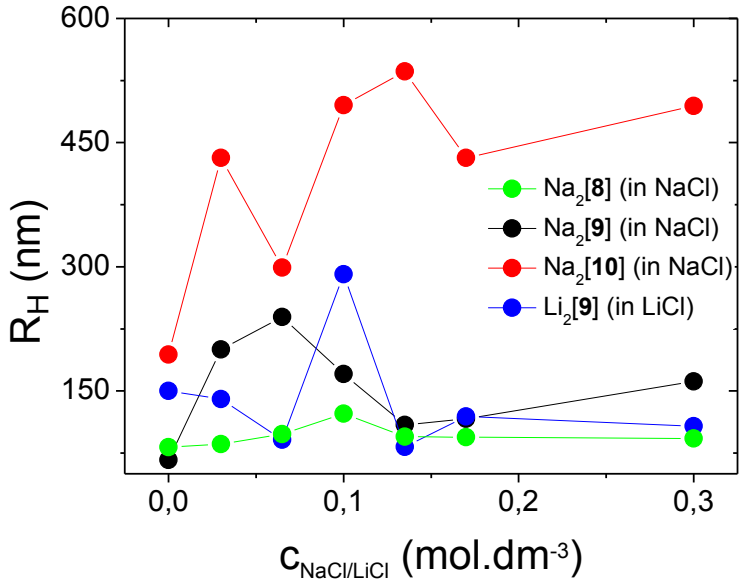

Figure 10 Dependence of the size of dumbbell aggregates on the salt concentration.

The comparison of R_H of saturated and half-diluted solutions of Na_2[**8**] is shown in Figure 11. Increase of size of particles with dilution is obvious. Interestingly there seems to be a steep increase of R_H when salt concentration is higher than 0.1 M. It means that the change of salt concentration has greater influence on dilute dumbbell solution.

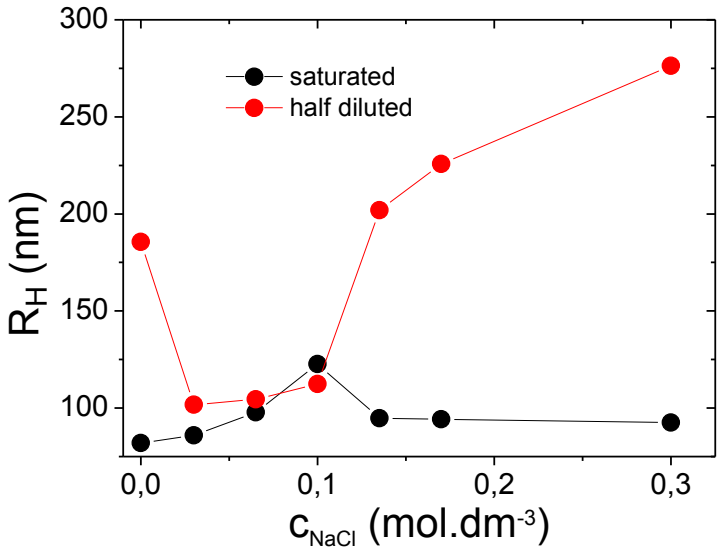

Figure 11 Dependence of R_H of Na_2[**8**] particles on NaCl concentration.

4.2 Cobalt bis(dicarbollide) anion in solutions with polymers

4.2.1 Cobalt bis(dicarbollide) anion and diblock copolymer PEO-PEOX

My bachelor thesis was focused on aqueous mixtures containing metallacarborane Na[**1**] and PEO-PEOX. One of the main results was the fact that the homopolymer poly(2-ethyl oxazoline), PEOX, interacts with Na[**1**]. PEOX and **1** formed the complex PEOX/**1,** which was soluble in water and NaCl solution. As described recently in literature, PEO also interacts with **1** and it forms insoluble complex PEO/**1**. The structure of this nanocomposite has been described in detail by quantum chemistry, WAXS and solid state NMR.[29] It was found earlier that the presence of salt influences strongly the interaction of cobalt bis(dicarbollide) with hydrophilic polymers (especially PEO-containing).[18] However, there is only slight dependence on NaCl concentration for PEOX homopolymer. Double hydrophilic copolymer PEO-PEOX was chosen to describe how **1** interacts with these blocks together. It was evident that the affinity of PEO-PEOX block copolymer to metallacarborane is strong. According the previous study of similar PEO/**1** complex it was assumed that ethylene groups of PEOX backbone interact with hydrogen atoms of boron clusters of **1** via dihydrogen bonds. The previous studies also showed that not only the dihydrogen bonds, but also the interaction of sodium counterion with PEO plays a significant role in the complex stabilization. Na^+ cations do not interact with amidic groups of the PEOX segments,[54] which is the reason why complex PEOX/**1** does not precipitate and it is water soluble.

The main result of bachelor thesis was the fact, that it is possible to prepare very stable spherical PEO-PEOX/**1** nanoparticles of rather unclear structure in salt solutions.

This diploma thesis continues in previous research to get deeper insight into the problem of aggregation of metallacarboranes, their interactions with polymers and the role of the counterions. For this purpose similar polymers of various architecture were chosen to compare differences in interaction of cobalt bis(dicarbollide) cluster with polymers in solutions of alkaline salts. Also other techniques were provided, such as small angle X-ray scattering (SAXS), NMR spectroscopy, and isothermal titration calorimetry (ITC) in order to reveal the inner structure of the nanospheres. Light scattering study was extended with results of titration in 0.154 M NaCl solution (physiological condition) and higher concentrations of **1**.

STATIC AND DYNAMIC LIGHT SCATTERING

The hybrid nanoparticles were prepared by a titration of PEO-PEOX dilute solutions (2 g/L) by Na[**1**]. The formation of aggregates was monitored by static and dynamic light scattering (SLS and DLS) during the titration in water and 0.01 M, 0.1 M and 0.154 M NaCl. Dependency of hydrodynamic radius (R_H), extrapolated to the zero scattering angle, on **1**-to-polymer segment ratio, ξ, (the sum of PEO and PEOX segments is taken into account) is shown in Figure 12. Since PEO-PEOX is a double hydrophilic block copolymer, scattering intensity of the pure copolymer solution is weak and it corresponds to the size of polymer coils (R_H around 3 nm). Also a small fraction of large aggregates was detected, as it was already described in introduction (Section 2.3.2). The addition of **1** leads to a steep increase of the scattering intensity. In Figures 12 we can distinguish two aggregation regions depending on ξ. In the first one (for $\xi <$ 0.05) DLS distribution of relaxation times is bimodal. Small particles with dimensions of few nanometers (probably the single PEO-PEOX chains) coexist with polydisperse and long-time unstable aggregates of size larger than 100 nm. A relatively low scattering intensity in this region suggests that the large aggregates are not compact particles and that their concentration is low which can be seen also from the distributions of relaxation times.

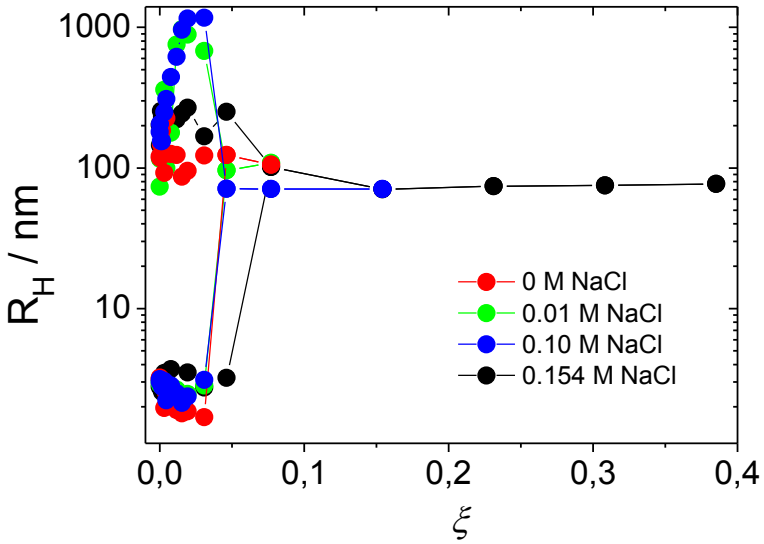

Figure 12 Dependence of hydrodynamic radius, R_H, on the addition of Na[**1**] to PEO-PEOX solution (2 g/L) in 0.00 M, 0.01 M and 0.154 M NaCl.

The scattering intensity rises steeply in the second region ($\xi > 0.05$) and it remains almost constant in 0.1 M and 0.154 M NaCl. However, other samples are unstable in this region and they precipitate. It is evident, that the nanoparticles in physiological saline and in 0.1 M NaCl (studied in detail in Bachelor thesis) are very similar. From the Zimm plot, the mass-average molar mass of the stable PEO-PEOX/**1** nanoparticles was evaluated ($\xi = 0.153$, dn/dc = 0.196 mL/g) and the following values were obtained: $M_w = 231 \times 10^6$ g/mol (PEO-PEOX aggregation number N^{agg} ca. 11 000; w(Na[**1**]) = 56 %). Their hydrodynamic radius obtained from the dynamic Zimm plot is 70 nm. Based on geometrical consideration, it was found that the overall density of presumably homogeneous spheres ρ(PEO-PEOX/**1**) is ca. 0.3 g/mL, which is a summation of two contributions: ρ(PEO-PEOX) = 0.15 g/mL and ρ(Na[**1**]) = 0.16 g/mL. It means that even though the large nanoparticles formed at $\xi > 0.05$ are more compact than those observed for $\xi < 0.05$, they still resemble gel-like particles.

Isothermal Calorimetry Titrations

To learn more about the thermodynamics of the co-assembly process the interaction of PEO, PEOX and PEO-PEOX with **1** was studied by ITC. The studied processes are exothermic in all three cases. In Figure 13 we can see the curves describing the titration of PEO-PEOX, which are very complex. The exothermic peak is bimodal in the region $0.25 < \xi < 1.5$. The first minimum occurs in the transition region between the first

unstable region and the formation of more stable spherical particles with R_H 70 nm. The second minimum is in a similar ξ range as the minimum for PEO (data not shown). We can see a small shift with salt concentration, but no significant differences between ITC curves for PEO-PEOX in solutions with increasing concentration of NaCl have been detected. From the comparison with the curves for PEOX/**1** and PEO/**1** (data now shown) we can suppose that the thermochemistry of PEOX-PEO/**1** formation is not a simple sum of PEOX/**1** and PEO/**1** contributions, and that there is a cooperation effect of PEO and PEOX segments. It supports the idea of binding of both blocks to one metallacarborane cluster and their mutual intermixing.

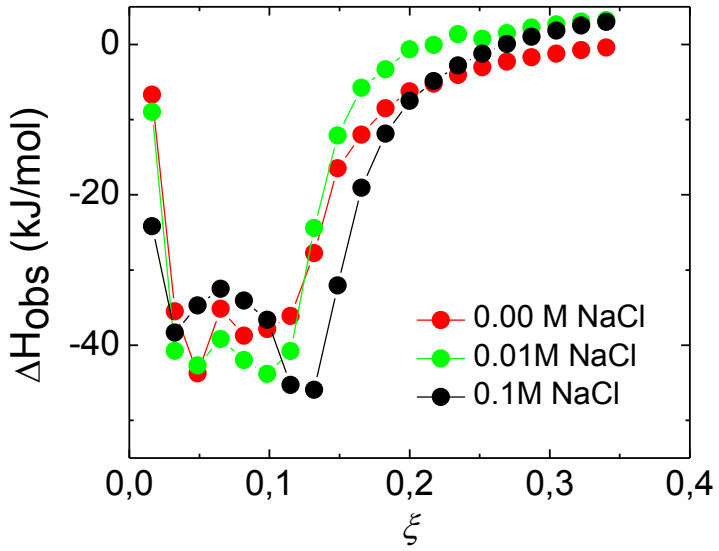

Figures 13 ITC thermogram for 0.0245 M Na[**1**] titrated into 0.5 g/L PEO-PEOX, in 0.00 M, 0.01 M and 0.10 M NaCl.

From the ITC data, the stoichiometry of the complex in 0.00 M, 0.01 M, and 0.10 M NaCl was calculated and the number of polymer segments interacting with one metallacarborane cluster was obtained: PEO: (6, 7, 12); PEOX: (6, 6, 5); PEO-PEOX: (7, 6, 6), respectively. From Figure 13 it is evident that the maximal loading capacity of the nanospheres in 0.1 M NaCl goes up to $\xi = 0.25$, which is equal to ca. 65% (w/w) of Na[**1**].

Small Angle X-ray Scattering

To get even more insight into the internal structure of nanoparticles, SAXS measurements on PEO-PEOX/**1** in 0.1 M NaCl with constant polymer concentration (10

g/L) and increasing ξ was performed. The SAXS measurements were used for investigation of the PEO-PEOX/**1** internal structure only. The scattering contrasts, based on specific volumes (measured earlier for Na[**1**] and PEO),[18] for all three components are comparable (almost equal for PEO and **1**, and slightly lower for PEOX).

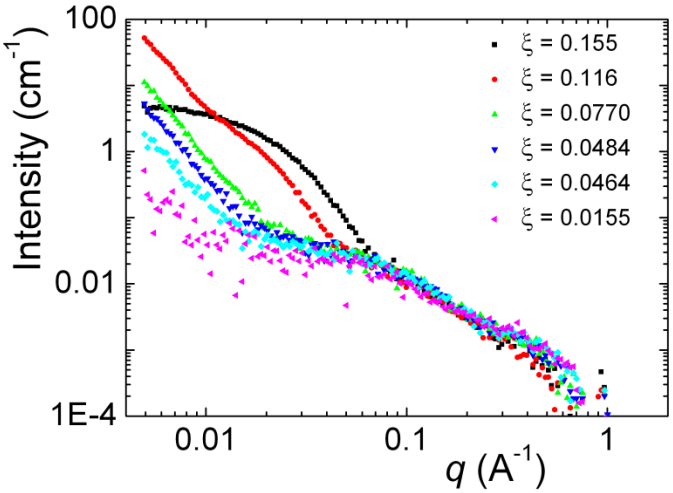

Figure 14 SAXS curves of 200 μL 10 g/L PEO-PEOX in 0.1 M NaCl after addition of 20 μL, 15 μL, 10 μL, 7.5 μL, 6 μL and 2 μL of 0.0245 M Na[**1**]. The corresponding values of ξ are also shown.

The SAXS curves are shown in Figure 14. Scattering curve behavior at higher angles (q around 0.1 Å^{-1}) indicates the presence of highly swollen chains, which can coexist as free chains in the solution and as a part of internal structure of the large particles. The experimental points for all the samples are the same in this region, but the situation significantly changes for lower angles. It is possible only in the case, when the block copolymer PEO-PEOX remains swollen giving the stable scattering signal at higher angles. At low ξ values, metallacarborane can be randomly distributed within the large objects. Above the critical ξ value ($\geq$ 0.116), Na[**1**] molecules can associate in small regions[55] inside the large swollen particles. Compact particles with sizes in the range of 10^1 nm in this ξ region were also confirmed by DLS measurements and other methods. The shape of the scattering curves with $\xi = 0.0464$ up to 0.116 indicates the presence of very large particles, the size of which is not possible to evaluate by SAXS.

However, the most important observation made by SAXS is the fact that there is no sign of any correlation peak in the region of high q between 0.1 and 1.0 Å^{-1}. The higher organized structures of metallacarborane clusters as well as polymer coils and their collapsed domains have not been proven in the studied system. It supports the

assumption of intermixing of PEO and PEOX blocks and a gel-like nature of the nanospheres.

NMR STUDY

We used ^{1}H NMR to estimate the fraction of polymer segments involved in the complex with different ξ and salt concentrations. In Figure 15, we show ^{1}H NMR spectrum of pure PEO-PEOX and the PEO-PEOX/**1** complex in 0.1 M NaCl with ξ = 0.045. It is evident that the peaks corresponding to hydrogen nuclei from PEOX (ethylene sub-unit 3.5 ppm; ethyl side-group $C\underline{H}_2CH_3$ 2.4 ppm and $CH_2C\underline{H}_3$ 1.1 ppm) are broad in the spectrum of PEO-PEOX/**1**. It indicates a restricted mobility of the parts of PEOX chains, which are engaged in the complex formation. The PEO/**1** segments are completely frozen, they do not contribute to the overall PEO signal and it is not therefore broadened. The ratios of integrated intensities of signals of ethylene sub-units in PEO (round 3.7 ppm) and PEOX blocks to those in a molecularly dissolved copolymer of the same concentration, which give the fractions of kinetically frozen monomer units, are shown in Inserts of Figure 15, respectively, as a function of ξ (0.015 and 0.045). It is evident that the fraction of "frozen" PEOX backbones is appreciably higher (25% and 40%, for increasing ξ) than that of PEO units (5% and 20%, for increasing ξ). In both cases, it increases with ξ and almost does not depend on the presence of salt. Right Insert in Figure 15 shows the fraction of kinetically frozen pending ethyl groups in the PEOX blocks (9% and 10%, for increasing ξ). We can see that their mobility does not depend on NaCl concentration and it is much less affected by the content of **1**. It indicates that the mobility of the entire PEOX/**1** segment is in fact higher than one would have expected from the immobilization of the ethylene sub-units. It confirms our assumptions that metallacarborane interacts directly with the backbone of PEOX via dihydrogen bonds.

Assuming that both components are involved in the complex formation, we can calculate from the NMR results the following: One copolymer chain consists of 114 PEO segments and 66 PEOX segments (see Scheme 3). One PEO_{114}-$PEOX_{66}$ chain interacts with ca. 3 molecules of Na[**1**] (ξ = 0.015), or ca. 8 molecules of Na[**1**] (ξ = 0.045). For ξ = 0.015, we obtained the following numbers of segments per polymer chain: 6 frozen PEO segments and 17 frozen PEOX "backbones", where only 6 from 17 PEOX segments involved in interaction with **1** are entirely frozen; For ξ = 0.045: 23

frozen PEO segments and 26 frozen PEOX "backbones", where only 7 from 26 PEOX segments involved in interaction with **1** are entirely frozen. Assuming that only frozen segments are involved in the complex formation, there are 6-8 polymer segments involved in the complex formation per one metallacarborane molecule almost regardless of NaCl and **1** concentration. All the data suggest that there are still sufficiently large amount of mobile segments that can stabilize the PEO-PEOX/**1** nanospheres in solution at high ξ: 73% of segments are not involved in the complex formation and 83% of segments are mobile.

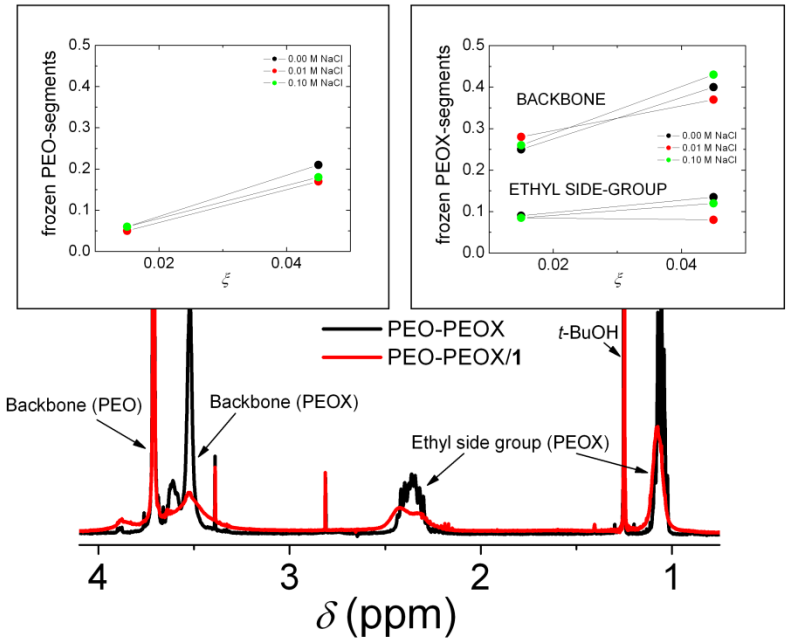

Figure 15 Typical ^{1}H NMR spectra of (black line) PEO-PEOX and (red line) PEO-PEOX/**1** (ξ = 0.045; 0.1 M NaCl) with *t*-butanol as an internal standard.
Inset: Fraction of frozen segments of PEO (left) and PEOX (right) in PEO-PEOX/**1** differing in Na[**1**] content and NaCl concentration calculated from a decrease of corresponding 1H NMR signals related to pure PEO-PEOX and *t*-butanol.

4.2.2 Different polymers solutions titrated by cobalt bis(dicarbollide)

The titration experiments with other copolymers containing both PEO and POX blocks were performed to extend understanding of interaction between the copolymer blocks and metallacarborane. We monitored the formation of aggregates by SLS and DLS during the titration of linear diblock PEO-PEOX, linear triblock PEOX-PEO-PEOX and 4-arm diblock PEO-PMOX (c = 2 g/L) by Na[**1**] (concentration of Na[**1**] was adjusted to get the same **1**-to-polymer segment ratio ξ for all three cases). All samples were

measured in 0.154 M NaCl. Dependencies of SLS intensity and hydrodynamic radii (R_H) are shown in Figures 16 and 17, respectively. At low concentration of **1** the increase of the scattering intensity is similar in case of the solutions of diblock and triblock copolymer. However, the curve of scattering intensity in the solution of 4-arm PEO-PMOX is different. Intensity at lower ratio ξ is higher than in the case of other two polymers. In the region of higher concentration of **1** (ξ > 0.05) the scattering intensity remains almost the same and it is lower than the intensity of diblock and triblock copolymer. These results correlate with the ratio of POX and PEO segments and with the architecture of corresponding copolymers. The high value of LS intensity means that large number of polymer chains is necessary to stabilize the complex in solution. PEO-PEOX diblock has 1.7-times higher content of PEO segments than PEOX ones, while triblock PEOX-PEO-PEOX has an equal number of both PEO and PEOX. Keeping in mind that PEOX/**1** complex is water-soluble and PEO/**1** is not, higher aggregation number for diblock is expected as compared to triblock copolymer, which manifests itself in the highest LS-intensity for PEO-PEOX/**1**. In the case of 4-arm copolymer, the PEO/PMOX ratio is 1.4:1. However, PMOX is more hydrophilic than PEOX. Furthermore, we observed for similar samples that the star-like architecture stabilizes insoluble polymer/metallacarborane complexes more efficiently than simple linear polymers.[56]

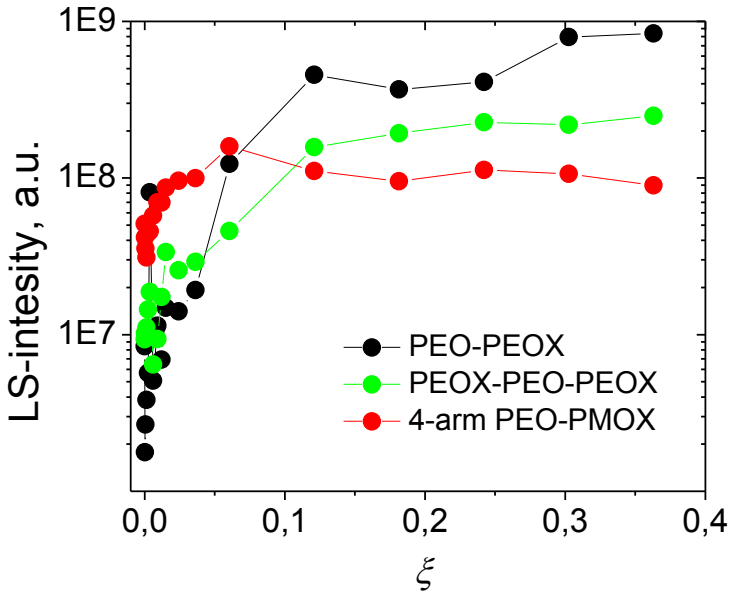

Figure 16 Dependence of light scattering intensity on the addition of Na[**1**] to PEO-PEOX, PEOX-PEO-PEOX and 4-arm PEO-PMOX solution (2 g/L) in 0.154 M NaCl.

In Figure 17 we can see that the largest particles with R_H around 120 nm were detected in the solution of triblock copolymer at high ξ, which also corresponds to the longest length of its polymeric chain. Shorter diblock copolymer PEO-PEOX forms smaller particles of size around 70 nm as was already discussed in Section 4.2.1. In solution of PEOX-PEO-PEOX we can also distinguish two regions as in case of PEO-PEOX solution. The process of aggregation in the solution of 4-arm PEO-PMOX with **1** is again different; only one type of particles was detected from the beginning of the titration and the hydrodynamic radius of particles is decreasing with addition of **1**. In the region with higher content of **1** (ξ > 0.1), particles of hydrodynamic radius only around 20 nm were detected. The solution of 4-arm PEO-PMOX in 0.154 M NaCl was also measured without addition of metallacarborane and small particles of size 3 nm were detected by DLS. These particles were not detected in the solution with added **1** while the solutions of PEO-PEOX or PEOX-PEO-PEOX contained also small 3nm particles. It indicates that 4-arm polymer probably exhibits higher affinity to metallacarborane at lower concentration of **1** to compare with linear copolymers and whole aggregation process is probably different. It is probably related with the compact architecture of star polymer as compared to lose linear chains.

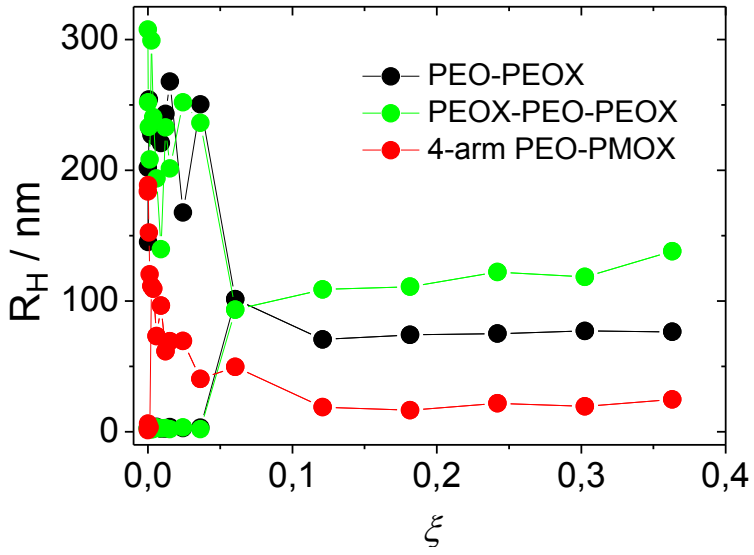

Figure 17 Dependence of hydrodynamic radius, R_H, on the addition of Na[**1**] to PEO-PEOX, PEOX-PEO-PEOX and 4-arm PEO-PMOX solution (2 g/L) in 0.154 M NaCl.

4.2.3 Influence of cations on aggregation

The same titration experiments as in previous part were carried out for diblock copolymer PEO-PEOX in chloride solutions of different cations to learn how the counterions influence the process of complexation of polymers with **1**. Results of DLS measurements of nanoparticles in PEO-PEOX solutions of 0.154M NaCl, LiCl and KCl titrated by Na[**1**] are shown in Figure 18. The behavior of titrated solutions of NaCl and LiCl seems to be very similar, from bimodal distribution of relaxation times it becomes monomodal at ratio ξ ca. 0.05. Surprisingly distribution of potassium salt solution is monomodal from the beginning of the titration. The size of particles is increasing with addition of **1** and in the region with $\xi > 0.005$ hydrodynamic radius stays stable around 100 - 120 nm. The reason of this exceptional behavior is still not clear. However, different theoretical binding energy of K^+ to PEO oligomers (Section 2.4.2) and larger diameter of potassium atom probably cause formation of larger nanoparticles in KCl solution.

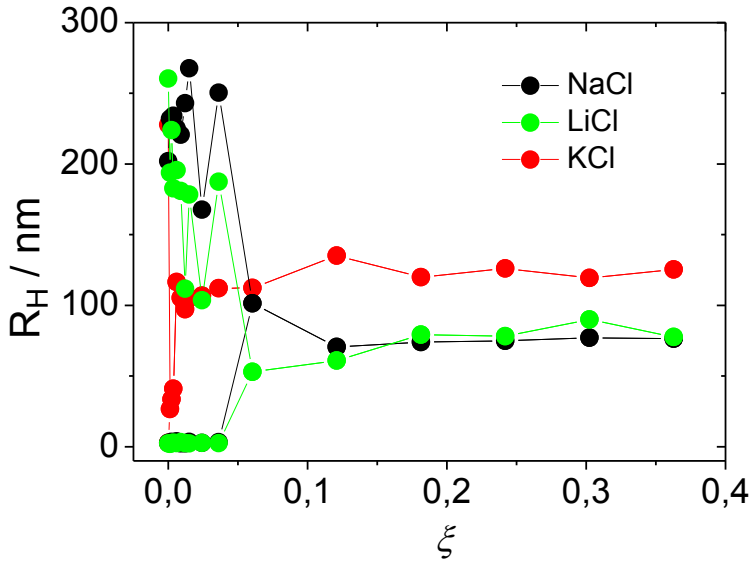

Figure 18 Addition of Na[**1**] (c = 0,019 M) in 0.154M NaCl, LiCl and KCl with PEO-PEOX (2g/L) to 0.154M NaCl, LiCl and KCl solution.

4.3 Conjugates of cobalt bis(dicarbollide) in solutions with polymers

In this part of study, conjugates with two cobalt bis(dicarbollide) clusters were examined. One of the reasons of this study is the application of results and ideas described in previous parts towards a drug-delivery of boron cluster compounds. Some

of these metallacarborane conjugates are known as inhibitors of HIV protease. The question was, whether polymers would interact also with double-cluster conjugates. In next paragraphs two types of conjugates are studied. The first are inhibitors, which were studied and also prepared in close relation with biochemical research of inhibition of HIV protease and other enzymes. Most of these compounds contain two clusters connected by PEG linker with amino group in the middle bounding different side chains or characteristic groups. Second group of studied metallacarborane compounds is called dumbbells according to their specific shape. Two clusters are connected by PEG linker differing in length and by a presence of *p*-phenylene subunit in the middle of the PEG linker. Since dumbbells compounds were prepared recently, the characteristics of their aqueous solutions have not been described as deeply as the solutions of the inhibitors compounds in the literature. Therefore the study of dumbbell compounds in this diploma thesis is much more detailed. The characterization of the solution behavior was provided by spectroscopy and light scattering measurements.

4.3.1 Inhibitors of HIV protease with PEO-PEOX

The structures of the studied inhibitors **2** – **7** are shown in Scheme 1. Almost all of them are sparingly soluble in water (**7** is an only exception because of the presence of charged and highly soluble borane cluster attached to the linker) and they form ill-defined aggregates in aqueous solutions, which is typical for almost all metallacarborane conjugates. The solubility is even lower in salted solutions due to a common-ion effect (it drops at least ten-times for all the inhibitors except **7**). An increase of solubility of the inhibitors was determined after the addition of 10 g/L PEOX-PEO in 0.154 M NaCl solution. The results are summarized in Table 2 together with hydrodynamic radii, R_H, of the corresponding aggregates and nanoparticles. From the high increase of solubility (ca. 10 times in average) and formation of nanoparticles with lower dimensions as compared to the aggregates of pure inhibitors, it is evident that PEO-PEOX interacts with all the inhibitors. The topology of the nanoparticles was also examined by AFM (data not shown). Generally it was found that the nanoparticles are of spherical shape and similar to PEO-PEOX/**1** nanospheres.

Recently, the inhibition activity against HIV protease of several compounds in presence of PEO-PEOX was also studied *in vitro*. The results revealed that the inhibitors have too high affinity to PEO-PEOX, which deteriorates their binding to HIV protease. Therefore the possible part of further research will be searching for suitable

method of releasing metallacarboranes from their complexes with polymers. One of the studied methods of releasing metallacarboranes was changing of salt concentration.

Table 2 Solubility increase and changes in hydrodynamic radii, R_H, of inhibitors after addition of PEO-PEOX in 0.154 M NaCl.

Compound	Absorbance increase at λ 300 nm	R_h / nm Inhibitor	R_h / nm Inhibitor + polymer
2	9-times	235	152
3	21-times	627	138
4	3-times	531	114
5	11-times	511	114
6	4-times	550	168
7	-	197	24

4.3.2 DUMBBELLS WITH PEO-PEOX, PEOX-PEO-PEOX AND 4-ARM PEO-PMOX

SOLUBILITY IN AQUEOUS AND SALT SOLUTIONS

In Section 4.1.1 solubility of pure dumbbells in aqueous or salt solutions was studied. This part is focused on the solubility of dumbbells in solution with PEO-PEOX, PEOX-PEO-PEOX, and 4-arm PEO-PMOX block copolymers in order to at least partly quantify the interaction of dumbbells with particular copolymers in solutions of three different alkaline cations (Li, Na and K). Solubility of dumbbells solutions with polymers (c = 10 g/L) was compared to corresponding salt solutions (0.154 M) without polymer by increasing of absorbance. In Figure 19 we can see the differences for sodium, lithium and potassium dumbbells solutions. Addition of polymers increased solubility in almost all cases as we expected from the solubility of inhibitor analogues. It means that the presence of polymers helps to disperse metallacarboranes in form of nanoparticles in most cases. The only exception is Li_2[**8**] in which we observed ca. 5 times lower solubility in polymer solutions to compare with those without polymer. It can be explained by the fact that the polymer/dumbbell complex is insoluble in this case. Increase of solubility of sodium samples is similar for Na_2[**8**], Na_2[**9**] and Na_2[**11**] (ca. 3 – 10 times). Solubility of Na_2[**10**] in polymer solutions is different and the increase of solubility is 25 times higher. The change in solubility of Li_2[**9**], Li_2[**10**] and

Li_2[**11**] is very similar to sodium ones. The highest increase of solubility was observed for potassium dumbbells. The increase of solubility is increasing roughly in the following sequence: $S_{K2[\mathbf{8}]} < S_{K2[\mathbf{9}]} < S_{K2[\mathbf{10}]} < S_{K2[\mathbf{11}]}$. In average, the solubility of dumbbells solutions in PEO-PEOX is lower for many cases than those in triblock PEOX-PEO-PEOX and 4-arm PEO-PMOX solutions. However, the differences are not such significant, and no simple trend has been found.

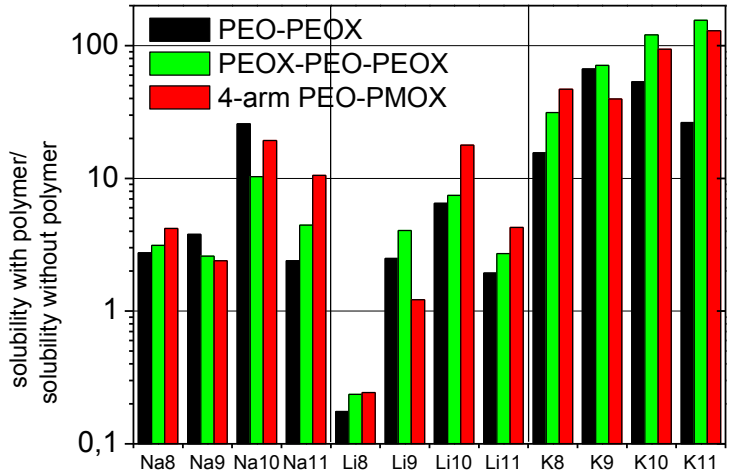

Figure 19 Solubility in 0.154 M salt solution with polymer (10 g/L) relative to that without polymer.

LIGHT SCATTERING

Saturated solutions of dumbbells with and without polymers described in the previous paragraph were characterized by DLS measurements at scattering angle 90°. Hydrodynamic radii of particles in pure salt solutions were compared to the samples with added polymer (Figure 20). Pure salt solutions of sodium and potassium dumbbells contained large aggregates only. In polymer solutions the decrease of R_H was observed in every sodium and potassium sample (4-7 times lower to compare with pure dumbbell solution). Lithium samples differ by their bimodal distribution of relaxation times. Small particles of size ca. 3 nm were observed in pure salt solution of Li_2[**8**] as it was already described in Section 4.1.2. In other lithium dumbbells solutions with PEO-PEOX and PEOX-PEO-PEOX great fraction of these small 3-5 nm particles was still present (not shown in graph), coexisting with large ones. In the solution of lithium dumbbells with 4-arm PEO-PMOX, nanoparticles of size 20 – 80 nm were observed

together with larger particles of size hundreds of nanometers (R_H of small particles not shown in graph). Small 3 nm particles were also detected in the solutions of Na_2[**8**] and Na_2[**9**] with PEOX-PEO-PEOX. There seems to be no significant trend in size of particles with change of added polymer. The most different R_H values for different polymers were observed in lithium samples.

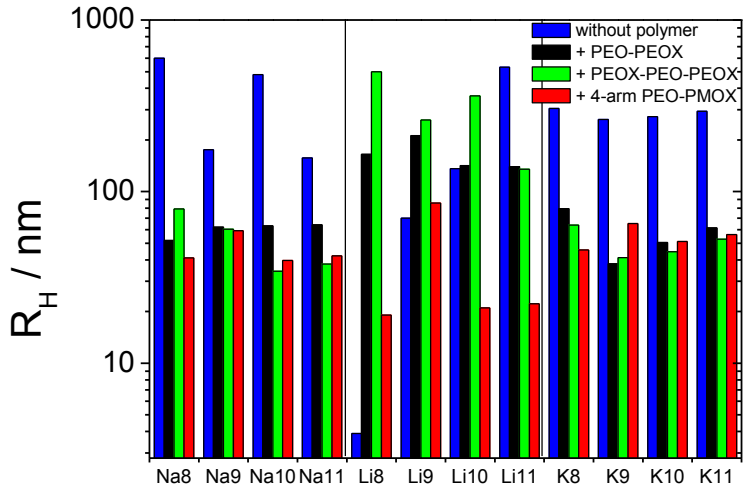

Figure 20 Size of the aggregates in saturated solutions of pure dumbbells compared to those with added polymer. All solutions are 0.154 M salt with corresponding counterion (NaCl, LiCl, KCl).

The solutions of dumbbells were studied by SLS and DLS after addition of salt solution of polymers PEO-PEOX, PEOX-PEO-PEOX and 4-arm PEO-PMOX (20 g/L). In comparison with the previous studies of Na[**1**]**,** we have to keep in mind that in this case the titration was carried out oppositely. Due to lower solubility of dumbbells in water and salt solution, polymer was added to metallacarborane solutions (dispersions) in 0.154 M salt, and therefore the ratio $1/\xi$ is used instead of ξ. All titrated solutions contained more than one type of particles and it was often difficult task to evaluate DLS data and to obtain accurate R_H values. It was even more complicated to get any reliable information from results of scattering intensity.

In Figure 21 we can see the dependence of hydrodynamic radius of Na_2[**8**] particles on addition of PEO-PEOX in 0.154 M NaCl. In this system three types of nanoparticles were observed for the entire $1/\xi$ range. Distribution of relaxation times of Na_2[**8**] solution titrated by PEOX-PEO-PEOX and 4-arm PEO-PMOX was also multimodal, presence of two types of particles (for some additions and scattering angles

even three types) were detected. In Figure 21 we can also see multimodal distribution of relaxation times after the last addition of polymer ($1/\xi$ = 750). In all the solutions the fraction of the fast mode (corresponding to 2-10 nm nanoparticles) was less than 8%. In the solution with added triblock PEOX-PEO-PEOX the fraction of the fast mode, which corresponds to smaller particles, was gradually increasing with addition of polymer up to ca. 40%. The fractions of the slow modes were very variable. There is no significant brake in the dependence, which could be related to the change of nanoparticle morphology and eventual saturation during the titration.

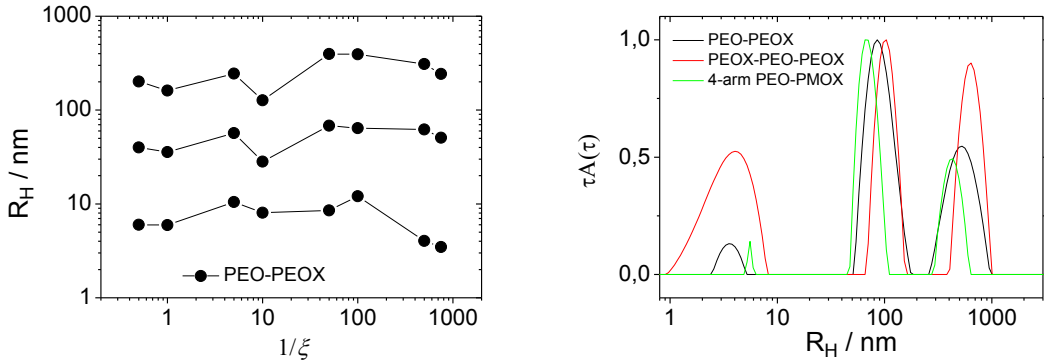

Figure 21 Left: Dependence of hydrodynamic radius, R_H, on the addition of diblock polymer PEO-PEOX (20 g/L) to Na_2[**8**] in 0.154M NaCl.
Right: DLS correlation spectra of Na_2[**8**] aggregates after addition of PEO-PEOX, PEOX-PEO-PEOX and 4-arm PEO-PMOX ($1/\xi$ = 750), all in 0.154M NaCl.

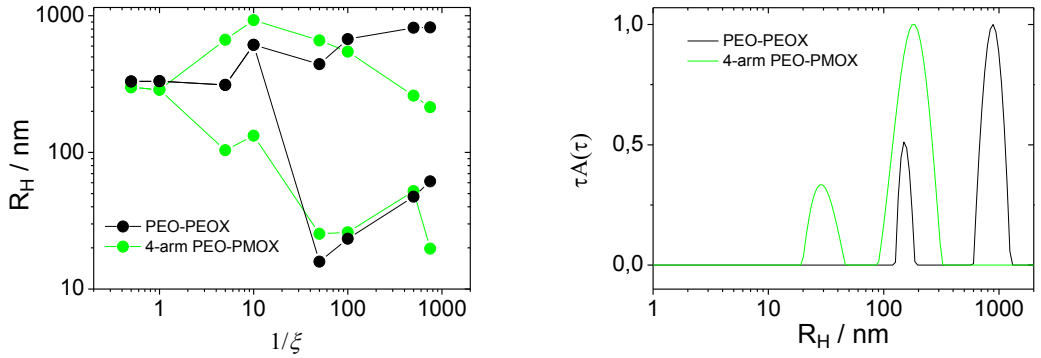

Figure 22 Left: Dependence of hydrodynamic radius, R_H, on the addition of diblock PEO-PEOX and 4-arm PEO-PMOX (20 g/L) to Li_2[**8**] in 0.154M LiCl solutions.
Right: DLS correlation spectra of Li_2[**8**] aggregates after addition of PEO-PEOX, PEOX-PEO-PEOX and 4-arm PEO-PMOX ($1/\xi$ = 750), all in 0.154M NaCl.

In Figure 22 we can see dependence of hydrodynamic radius of Li_2[**8**] particles on addition of polymers in 0.154 M LiCl. The solution of Li_2[**8**] titrated by triblock

PEOX-PEO-PEOX contained two or three types of particles and no significant trend in hydrodynamic radius or scattering intensity was observed. However, the solutions of diblock PEO-PEOX and 4-arm PEO-PMOX have some similarities in R_H dependency. Both solutions become bimodal for $1/\xi$ higher than 10 or 1, respectively. To compare this results with previous study of Na[**1**], we can easily recalculate the ratio ξ at the brake: for PEO-PEOX we get $\xi = 0.1$ and for 4-arm PEO-PMOX $\xi = 1$. It is obvious that at these breaks, the complex nanoparticles are saturated by the polymer and free polymeric chains are detected.

The same titration experiments were performed with 0.154 M KCl solutions of K_2[**8**] and results were again different from those in NaCl and LiCl. The solution titrated by triblock PEOX-PEO-PEOX contained three different types of particles (Figure 22). In the solution with added PEO-PEOX, similar change as in case of LiCl solutions with PEO-PEOX was observed. In this case, the addition of polymer, after which the smaller particles appeared, is around ξ 0.2. Behavior of 4-arm polymer is quite opposite and bimodal distribution of relaxation times becomes monomodal with particles of size from 110 to 180 nm. It also indicates that the change in morphology of nanoparticles occurred during the titration.

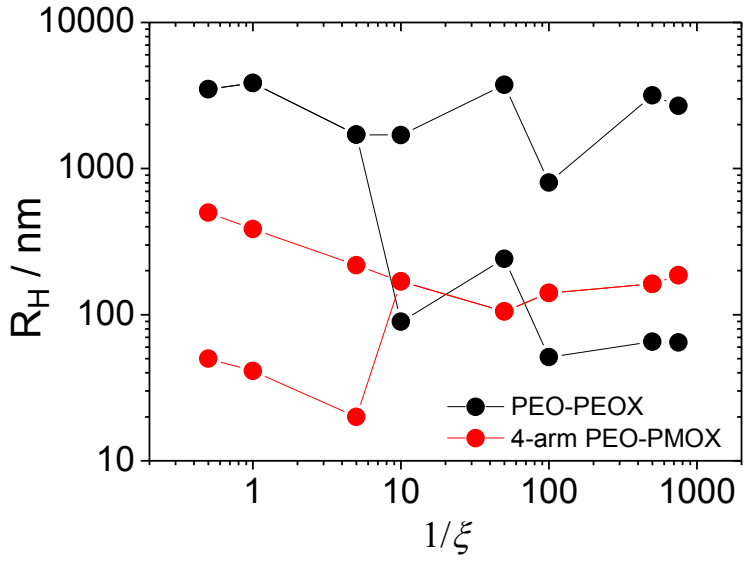

Figure 23 Dependence of hydrodynamic radius, R_H, on the addition of diblock PEO-PEOX and 4-arm PEO-PMOX (20 g/L) to K_2[**8**] (all in 0.154M KCl solutions).

5 SUMMARY

In the presented work behavior of cobalt bis(dicarbollide) anion, **1**, with potential utilization in a drug delivery of carboranes, and his conjugates (HIV inhibitors and dumbbells) was investigated.

Study of solubility of dumbbells showed that sodium and lithium dumbbells are the most soluble. The nature of the handle influences the value of pK_{sp}. In general, increasing length of the PEG linker causes lower solubility of samples and the presence of *p*-phenylene subunits in linker also affects solubility. Dihydroxybenzene group in the handle increases solubility, while dihydroxy-*p*-xylene group has the opposite effect. The impact of the handle became smaller for hydrogen and potassium dumbbells. They are both sparingly soluble. NMe_4^+ salts are the most insoluble and an influence of the handle is very low. The solubility of all the samples is lower in 0.154 M salt solutions. This is mainly due to the common ion effect.

In solutions of dumbbells large aggregates were detected by DLS. The only exceptions are solution of Na_2[**8**] with also small 2nm particles and Li_2[**8**], which contained 3nm particles only. Dependence of size on salt concentration did not show any significant trend.

In order to prepare and characterize novel hybrid nanoparticles containing **1**, we carried out a combined experimental study on PEO-PEOX/**1** mixtures differing in metallacarborane content and NaCl concentration. Both blocks interact with metallacarborane, and PEO-PEOX/**1** forms stable spherical nanoparticles in 0.1 M and 0.154 M NaCl aqueous solution (physiological saline) containing sufficiently high amount of **1**. Their inner structure does not exhibit a distinct core/shell structure. The multi-methodical study shows that both blocks are intermixed and cross-linked by **1**. These gel-like nanospheres are stabilized by hydrated free parts of both blocks and mainly by soluble PEOX/**1** segments bearing a negative charge. It means that much higher inhibitor loadings can be achieved in comparison with the case that the drug interacts with one block only. From ITC experiments, the loading capacity of PEO-PEOX/**1** nanospheres in 0.1 M NaCl is up to 65% (w/w) of Na[**1**].

An influence of polymers PEOX-PEO-PEOX and 4-arm PEO-PMOX was compared with PEO-PEOX and it was found, that PEO/PEOX ratio affects aggregation and the star-like architecture stabilizes polymer/metallacarborane complexes more

efficiently than simple linear polymers. 4-arm polymer exhibits higher affinity to metallacarborane at lower concentration of **1** to compare with linear copolymers and whole aggregation process is different resulting in relatively small hybrid nanoparticles.

Aggregation of **1** with PEO-PEOX was compared for NaCl, LiCl and KCl solution and it was found that aggregation in KCl solution differs by larger particles, which is probably caused by higher interaction energy between PEO and K^+ and larger diameter of potassium atom.

From the study of dumbbells and inhibitors it was found that solubility of both compounds increase with addition of polymers and the only exception is Li_2[**8**] with opposite effect. In most cases hydrodynamic radii of both types of conjugates decrease with addition of polymer. Lithium dumbbells contained 2 types of particles, including small 3nm ones. Titration of sodium, lithium and potassium dumbbells with polymers showed that aggregation process is complicated and unpredictable, system is often bimodal or even 3 modes are present.

6 REFERENCES

1. Casanova, J. (Ed.). *The borane, Carborane, Carbocation continuum*, John Wiley and Sons, Inc., New York, **1998**.
2. *Chem. Rev*. 92, **1992**, special issue on boranes and heteroboranes.
3. Grimes, R. N. *Coord. Chem. Rev*. **2000**, *200*, 773.
4. Hosmane, N. S.; Maguire, J. *Comments Inor.Chem.* **2005**, *26*, 183.
5. Custelcean, R.; Jackson, J. E. *Chem. Rev.* **2001**, *101*, 1963.
6. Gruner, B.; Plesek, J.; Baca, J.; Cisarova, I.; Dozol, J. F.; Rouquette, H.; Vinas, C.; Selucky, P.; Rais, *J. New J. Chem*., **2002**, *26*(10), 1519.
7. Gruner, B.; Kvicalova, M.; Plesek, J.; Sicha, V.; Cisarova, I.; Lucanikova, M.; Selucky, P. J. *Organomet. Chem*., **2009**, *694*(11), 1678.
8. Valliant, J. F.; Schaffer, P. J. *Inorg. Biochem.* **2001**, *85*(1), 43.
9. Tjarks, W. J. *Organomet. Chem*. **2000**, *614*, 37.
10. Valliant, J. F.; Guenther, K. J.; King, A. S.; Morel, P.; Schaffer, P.; Sogbein, O. O.; Stephenson, K. A. *Coord. Chem. Rev.*, **2002**, *232*(1-2), 173.
11. Armstrong, A. F.; Valliant, J. F. *Dalton Trans*., **2007**, *38*, 4240.
12. Cigler, P.; Kozisek, M.; Rezacova, P.; Brynda, J.; Otwinowski, Z.; Pokorna, J.; Plesek, J.; Gruner, B.; Doleckova-Maresova, L.; Masa, M.; Sedlacek, J.; Bodem, J.; Krausslich, H. G.; Kral, V.; Konvalinka, J. *Proc. Natl. Acad. Sci. U.S.A.* **2005**, *102*, 15394.
13. Scholz, M.; Bensdorf, K.; Gust, R.; Hey-Hawkins, E. *ChemMedChem*. **2009**, *4*(5), 746.
14. Fanfrlik, J.; Lepsik, M.; Horinek, D.; Havlas, Z.; Hobza, P. *Chem. Phys. Chem.* **2006**, *7*, 1100.
15. Kohl, N. E., Emini, E. A., Schleif, W. A., et al. *Proc. Natl. Acad. Sci. U. S. A.* **1988,** *85*, 4686.
16. Kozisek, M.; Cigler, P.; Lepsik, M.; Fanfrlik, J.; Rezacova, P.; Brynda, J.; Pokorna, J.; Plesek, J.; Gruner, B.; Grantz Saskova, K.; Vaclavikova, J.; Kral, V.; Konvalinka, J. *J. Med. Chem*. **2008**, *51*, 4839.
17. Matejicek, P.; Cigler, P.; Prochazka, K.; Kral, V. *Langmuir* **2006,** *22*, 575.
18. Matejicek, M.; Zednik, J.; Uselova, K.; Plestil, J.; Fanfrlik, J.; Nykanen, A.; Roukolainen, J.; Hobza, P.; Procházka, K. *Macromolecules* **2009**, *42*, 4829.

19. Matejicek, P.; Cigler, P.; Olejniczak, A. B.; Andrysiak, A.; Wojtczak, B.; Prochazka, K.; Lesnikowski, Z. J. *Langmuir* **2008**, *24*, 2625.
20. Kubat, P.; Lang, K., Cigler, P. et al. *J. Phys. Chem.* **2007**, *111*, 4539.
21. Uchman, M.; Cígler, P.; Gruner, B.; Procházka, K.; Matejíček, P. *J. Colloid Interface Sci.* **2010**, *348*, 129.
22. Rak, J.; Tkadlecovka, M.; Cigler, P.; Kral, V. *Chem. Listy* **2008**, *102*, 209.
23. Rak, J.; R. Kaplánek, V. Král, Bioorg. *Med. Chem. Lett.* **2010,** *20*, 1045.
24. Rais, J.; Gruner, B. In *Solvent Extraction*; Marcus, I., SenGupta, A. K. Eds.; Marcel Dekker: New York, 2005; p 243.
25. Henderson, W. A.; Brooks, N. R.; Young, V. G. *J. Am. Chem. Soc*. **2003**, *125*, 12098.
26. Lightfood, P.; Mehta, M. A.; Bruce, P. G. *J. Mater. Chem*. **1992**, *2*, 379.
27. Farras, P.; Teixidor, F.; Kivekas, R.; Sillanpaa, R.; Vinas, C.; Gruner, B.; Cisarova, I. *Inorg. Chem.* **2008**, *47*, 9497.
28. Fanfrlik, J.; Brynda, J.; Rezac, J.; Hobza, P.; Lepsik, M. *J. Phys. Chem. B* **2008**, *112*, 15094.
29. Matejicek, P.; Brus, J.; Jigounov, A.; Plestil, J.; Uchman, M.; Prochazka, K.; Gradzielski, M. *Macromolecules* **2011,** *44*, 3847.
30. Colfen, H. *Macromol. Rapid Commun*. **2001**, *22*, 219.
31. Alarcon, C. d. l. H.; Pennadam, S.; Alexander, C. *Chem. Soc. Rev*. **2005**, *34*, 276.
32. Lazzari, M.; Liu, G.; Lecommandoux, S. Block Copolymers in *Nanoscience*; Wiley: New York, 2006.
33. Cölfen, H.; Mann, S. *Angew. Chem., Int. Ed*. **2003**, *42*, 2350.
34. Ke, F.; Mo, X.; Yang, R.; Wang, Y.; Liang, D. *Macromolecules* **2009**, *42*, 5339.
35. Berlinova, I.; Iliev, N.; Vladimirov, P.; Novakov, C. *J. Polym. Sci., Part A: Polym. Chem.* **2007**, *45*, 4720.
36. Kjøniksen, A.-L.; Nyström, B.; Tenhu, H. *Colloids Surf., A* **2003**, *228*, 75.
37. Nedelcheva, A., N.; Vladimirov, N., G.; Novakov, C., P.; Berlinova, I., V. *J. Polym. Sci., Part A: Polym. Chem.* **2004**, *42*, 5736.
38. Casse, O.; Shkilnyy, A.; Linders, J.; Mayer, C.; Haussinger, D.; Volkel, A.; Thunemann, A. F.; Dimova, R.; Colfen, H.; Meier, W.; Schlaad, H.; Taubert, A. *Macromolecules* **2012**, *45*, 4772.
39. Gitsov, I.; Frechet, J. *J. Am. Chem. Soc.* **1996**, *118*, 3785.

40. Ihre, H; Hult, A; Soderlind, E. *J. Am. Chem. Soc.* **1996**, *118*, 6388.
41. Inoue, K. *Prog. Polym. Sci.* **2000**, *25*, 453.
42. Tomalia, D. A.; Sheetz, D. P. *J. Polym. Sci. Part A* **1966**, *4*, 2253.
43. Seeliger, W.; Aufderhaar, E.; Diepers, W.; Feinauer, R.; Nehring, R.; Thier, W.; Hellmann, H. *Angew. Chem.* **1966**, *78*, 913.
44. Adams, N.; Schubert, U. S. *Adv. Drug Delivery Rev*. **2007**, *59*, 1504.
45. Lin, P.; Clash, C.; Pearce, E. M.; Kwei, T. K.; Aponte, M. A. *J. Polym. Sci. Part B* **1988**, *26*, 603.
46. M. C. Woodle, C. M. Engbers, S. Zalipsky, *Bioconjugate Chem*. **1994**, *5*, 493.
47. Huber, S.; Hutter, N.; Jordan, R. *Colloid Polym. Sci.* **2008**, *286*, 1653.
48. Wang, C. H.; Fan, K. R.; Hsiue, G. H. *Biomaterials* **2005**, *26*, 2803.
49. Jeong, J. H.; Song, S. H.; Lim, D. W.; Lee, H.; Park, T. G. *J. Controlled Release* **2001**, *73*, 391.
50. Fenton, D.E.; Parker, J.M.; Wright, P.V. *Polymer* **1973**, *7*, 319.
51. Frech, R.; Huang, W. *Macromolecules* **1995**, *28*, 1246.
52. Dhumal, N. R.; Geji, S. P. *Chem. Phys.* **2006**, *323*, 595.
53. Consta, S.; Chung, J. K. *J. Phys. Chem. B* **2011**, *115*, 10447.
54. Okur, H. I.; Kherb, J.; Cremer, P. S. *J. Am. Chem. Soc.*, **2013**, *135*, 5062.
55. Rezacova, P.; Cigler, P.; Matejicek, P.; Lepsik, M.; Pokorna, J.; Gruner, B.; Konvalinka, J. Medicinal Application of Carboranes: Inhibition of HIV Protease. In *Boron Science: New Technologies and Applications*; Hosmane, N. S., Ed.; CRC Press: New York, 2011; pp 41.
56. Private communication of Pavel Matejicek.